

Figures to be held in the editorial files

(1)

Numerical analysis of gas-particle two-phase flows  
(Numerical Results)

By Ryuji Ishii, Yoshikuni Umeda and Masatoshi Yuhi

Department of Aeronautics, Kyoto University  
Yoshida Honmachi, Sakyo-ku, Kyoto 606, Japan

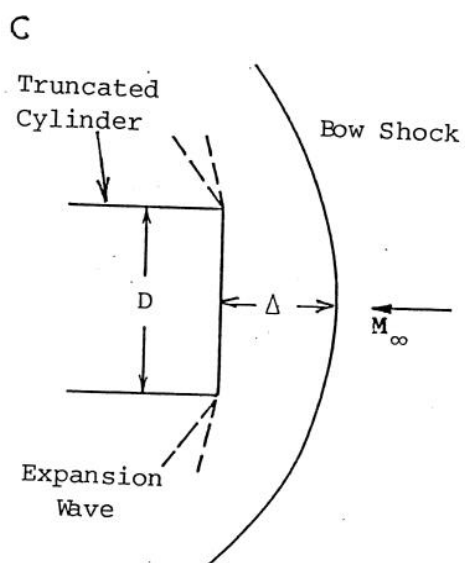
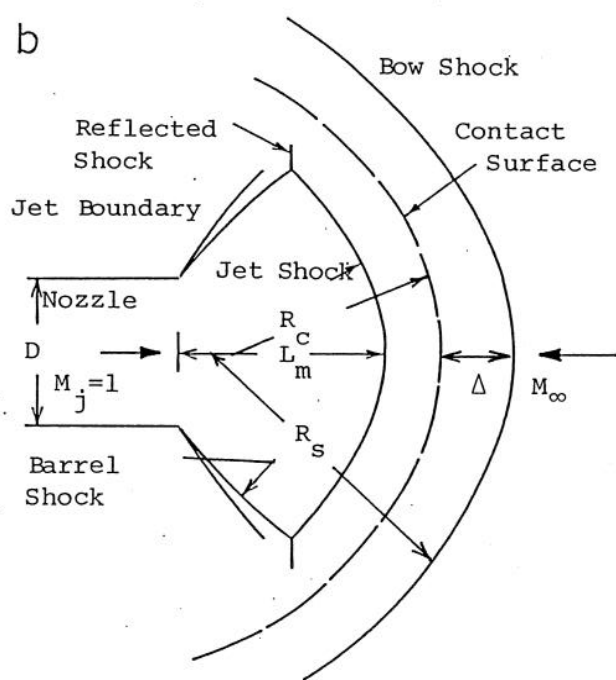
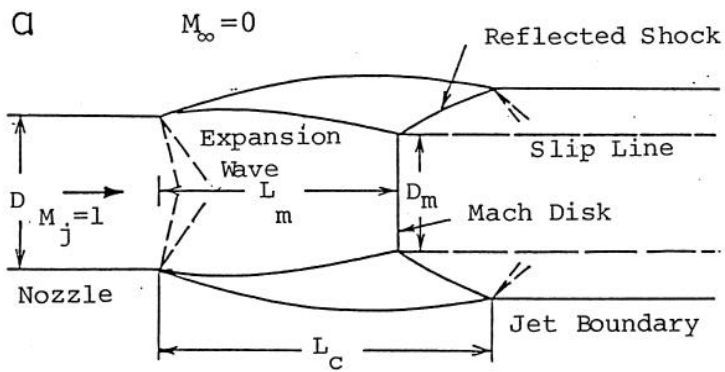
(2)

Table 1. Physical constants of gas and particles used in the numerical calculations.

Gas (Air)	Particles ( $\text{Al}_2\text{O}_3$ )
$\gamma = 1.4$	$\bar{\rho}_{\text{mp}} = 4.0 \times 10^3 \text{ kg/m}^3$
$\bar{C}_{pg} = 1005 \text{ J/kg.K}$	$\bar{C}_{pp} = 1686 \text{ J/kg.m}$
$\bar{\mu} = 1.79 \times 10^{-5} \text{ kg/m.s}$ (for $\bar{T} = 288 \text{ K}$ )	
$\delta = 0.5$	
$P_r = 0.75$	

(3)

## Calculated flowfields



## Figure captions

- B-1) Time history of density profile along the jet axis of a dust-free jet for  $\bar{p}_0/\bar{p}_\infty = 20$ . The jet begins to blow into a stagnant ambient gas region at  $t = 0$  ( $n = 0$ ). The flow Mach number of the jet at the nozzle exit is  $M_j = 1$ ;  $\Delta x = \Delta y = 0.1$ .
- B-2) Time history of density profile along the axis of a dust-free opposing jet for  $\bar{p}_0/\bar{p}_\infty = 20$ . The jet begins to blow opposing to a uniform mainstream ( $M_\infty = 2.0$ ) at  $t = 0$  ( $n=0$ ). The flow Mach number at the nozzle exit is  $M_j = 1.0$ ;  $\Delta x = \Delta y = 0.1$ .
- B-3) Time history of density profile along the body axis. A uniform supersonic flow ( $M_\infty = 2.0$ ) impinges on a truncated cylinder at time  $t = 0$  ( $n = 0$ );  $\Delta x = \Delta y = 0.02$ .
- B-4) Time history of density profile along the jet axis of a dusty jet;  $\bar{L} = 5 \text{ cm}$ ,  $\bar{p}_0 = 5 \text{ atm}$ ,  $\bar{p}_0/\bar{p}_\infty = 20$ ,  $\bar{T}_0 = \bar{T}_\infty = 290 \text{ K}$ ,  $M_j = 1.0$ ,  $M_\infty = 0$ ,  $\nu_j = 0.3$ ,  $\bar{r}_p = 1.0 \mu\text{m}$ ,  $\Delta x = \Delta y = 0.1$ ,  $K = 50$ ,  $F = 0.8$ . The particles are injected into the dust-free jet at the nozzle exit after  $n = 6000$ .
- B-5) Time history of density profile along the jet axis of a dusty opposing jet;  $\bar{L} = 5\text{cm}$ ,  $\bar{p}_0 = 5 \text{ atm}$ ,  $\bar{p}_0/\bar{p}_\infty = 20$ ,  $\bar{T}_0 = \bar{T}_\infty = 290 \text{ K}$ ,  $M_j = 1$ ,  $M_\infty = 2.0$ ,  $\nu_j = 0.3$ ,  $\bar{r}_p = 1.0 \mu\text{m}$ ,  $\Delta x = \Delta y = 0.1$ ,  $K = 50$ ,  $F = 0.8$ . The particles are injected into the dust-free jet at the nozzle exit after  $n = 9000$ .
- B-6) Time history of density profile along the body axis of a dusty supersonic flow around a truncated cylinder;  $\bar{L} = 5\text{cm}$ ,  $\bar{p}_\infty = 0.5 \text{ atm}$ ,  $\bar{T}_\infty = 290\text{K}$ ,  $M_\infty = 2$ ,  $\nu_\infty = 0.3$ ,  $\bar{r}_p = 2\mu\text{m}$ ,  $\Delta x = \Delta y = 0.05$ ,  $K = 250$ ,  $F = 0.8$ . The particles are injected into the dust-free flow at a plane perpendicular to the body axis ahead of the bow shock after  $n=4000$ .

(5)

- B-7) Velocity field of the dust-free jet shown in figure B-1.
- B-8) Velocity field of the dust-free opposing jet shown in figure B-2.
- B-9) Flow field of the dust-free supersonic flow around a truncated cylinder shown in figure B-3. These are obtained with finer mesh than those shown in the text.
- B-10) Particle trajectories in the jet shown in figure B-1.
- B-11) Particle trajectories in the opposing jet shown in figure B-2.
- B-12) Particle trajectories in the supersonic flow around a truncated cylinder shown in figure B-3.
- B-13) Velocity and temperature distributions along the jet axis of the dusty jet shown in figure B-4.
- B-14) Velocity and temperature distributions along the jet axis of dusty opposing jet shown in figure B-5.
- B-15) Distributions of flow quantities in the dusty shock layer shown in figure B-6:
  - a) Density distributions along the body axis.
  - b) Pressure distributions along the body axis.
  - c) Temperature distributions along the body axis.
  - d) Velocity distributions along the body axis.
  - e) Density distributions along the body wall.
  - f) Pressure distributions along the body wall.
- B-16) Constant density contours of particle phase in the dusty shock layer shown in figure B-6.
- B-17) Spatial distributions of particle clouds in the whole computational region for the dusty supersonic flow around a truncated cylinder shown in figure B-6.

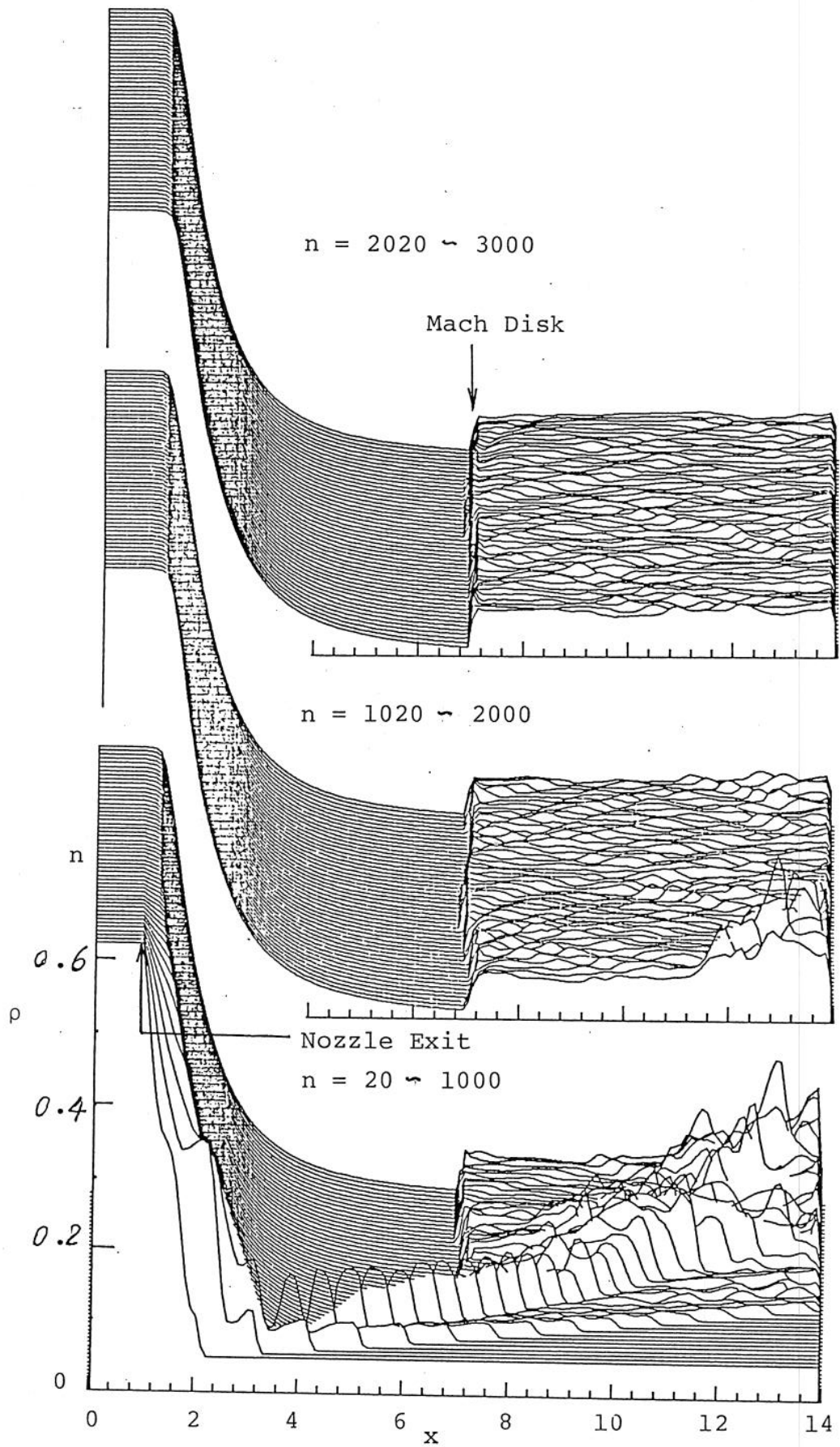


Fig. B-1 - 1

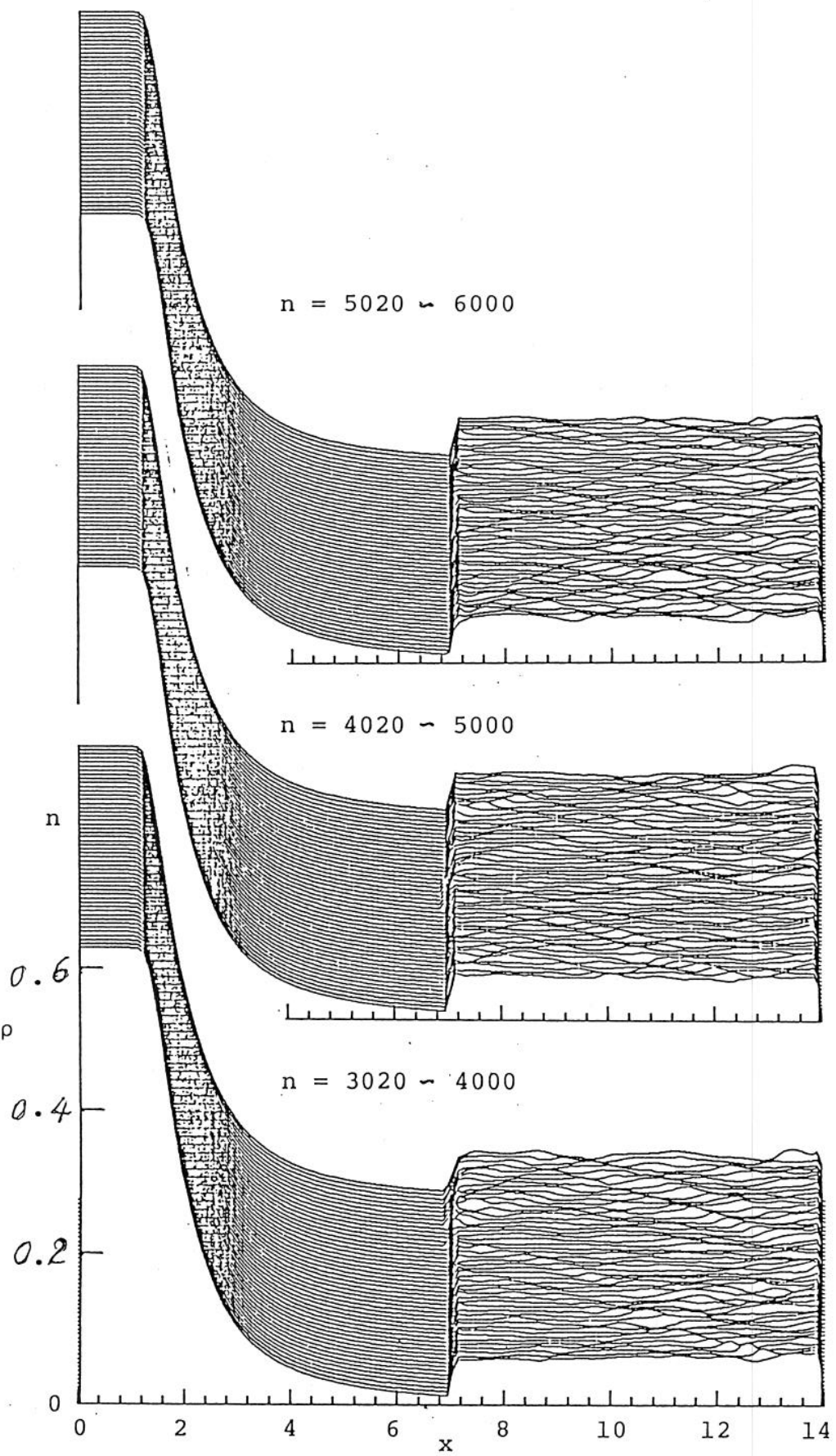


Fig. B-1 - 2

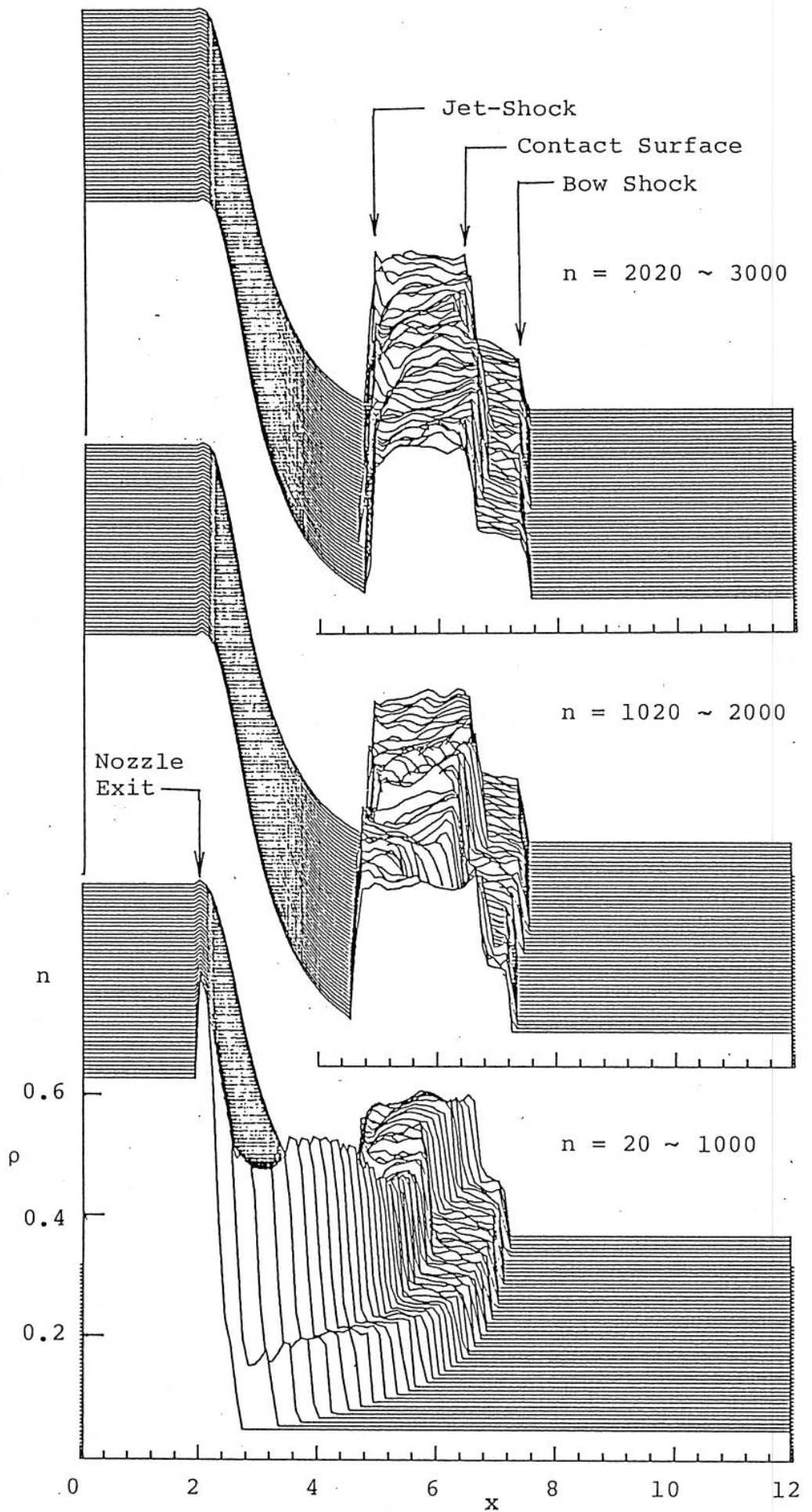


Fig. B-2 -1

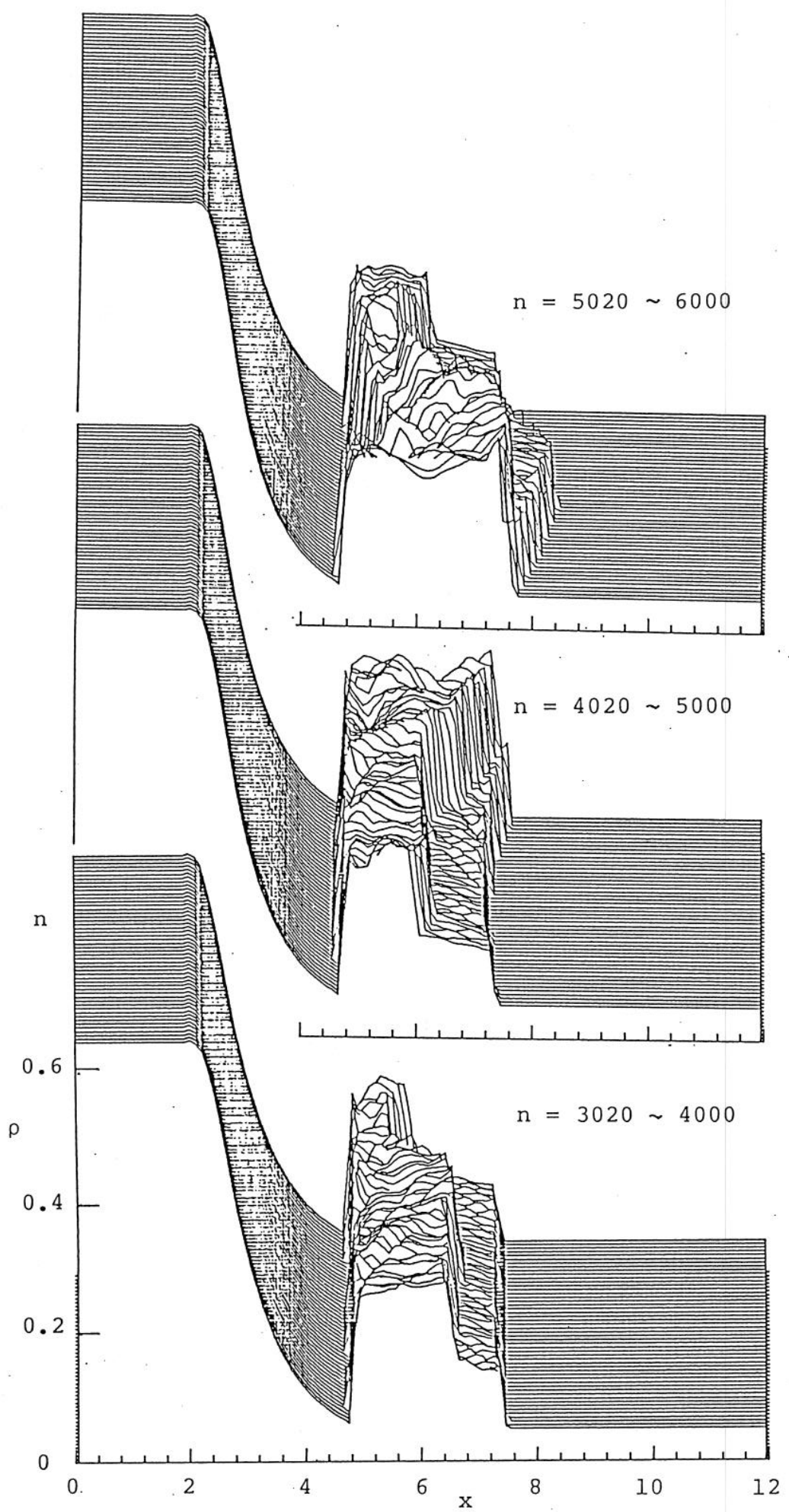


Fig. B-Z -2

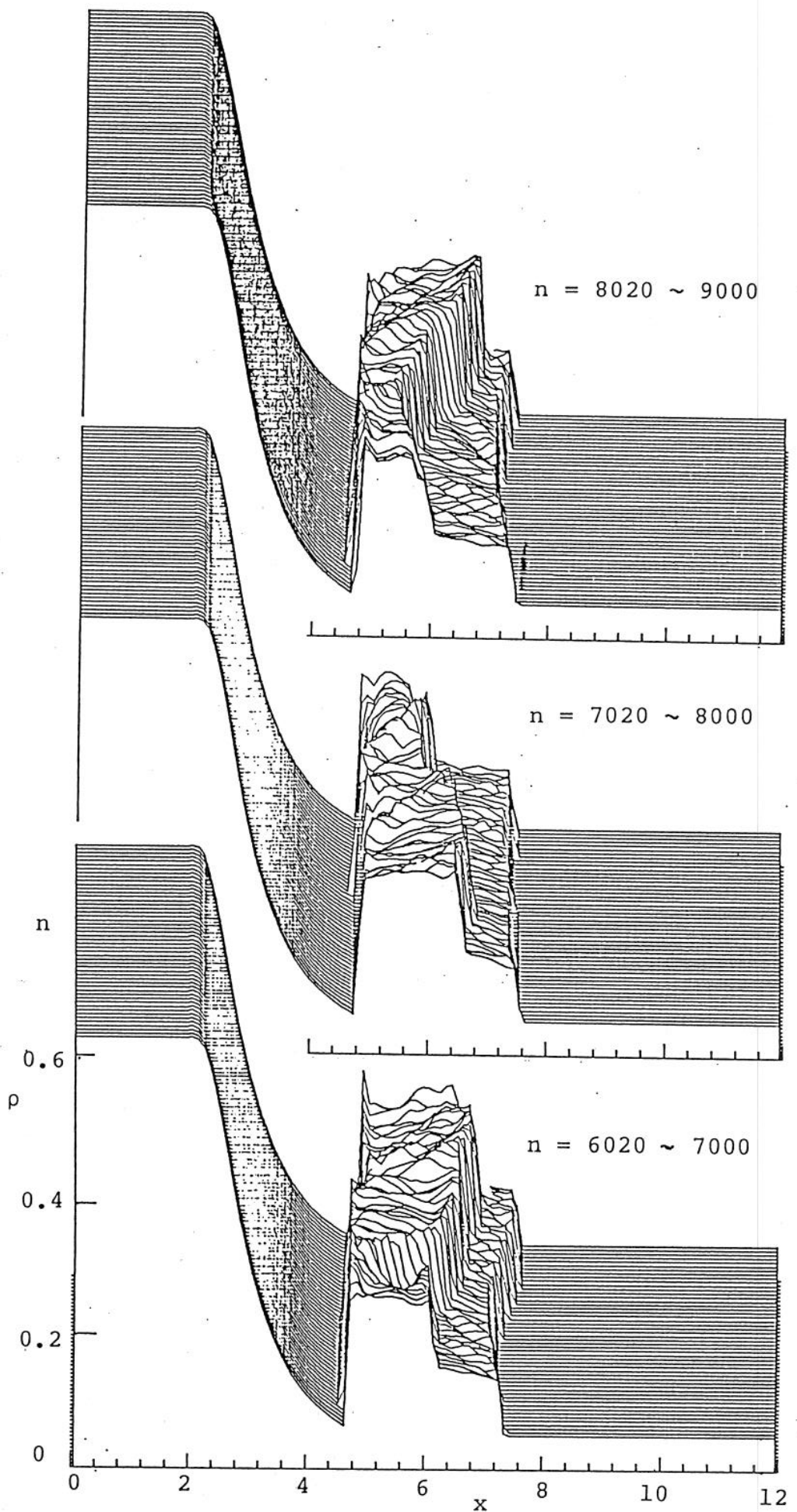


Fig. B-2 - 3

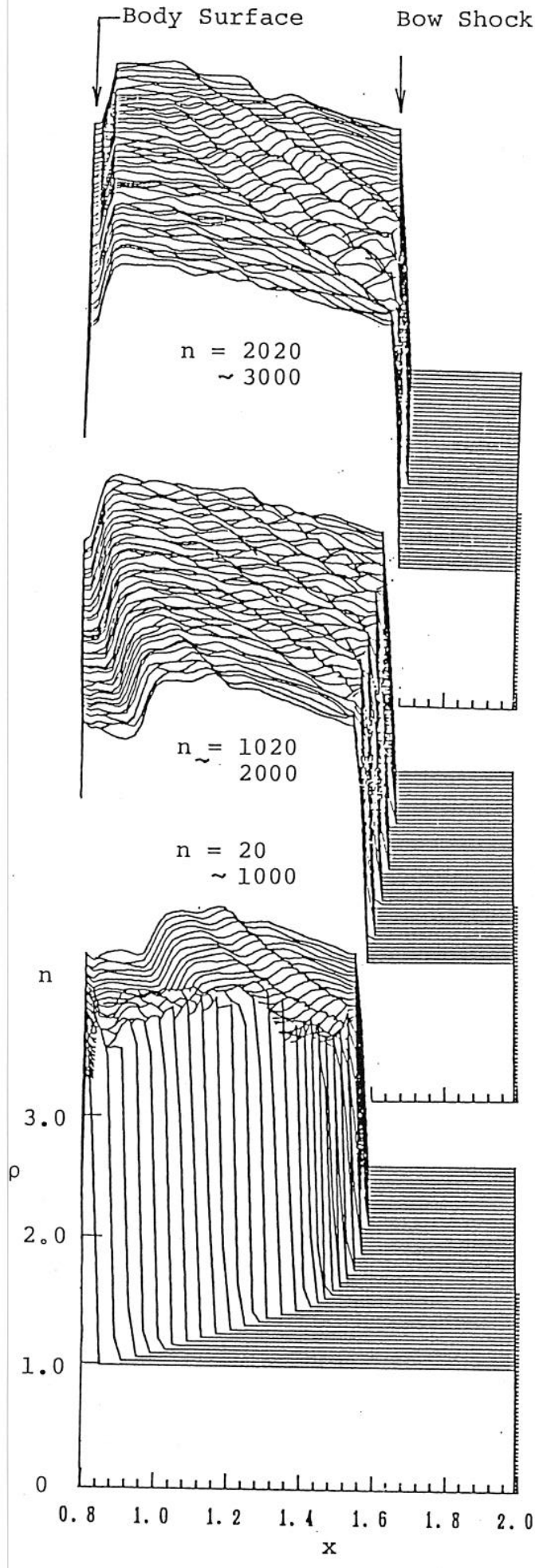


Fig. B-3

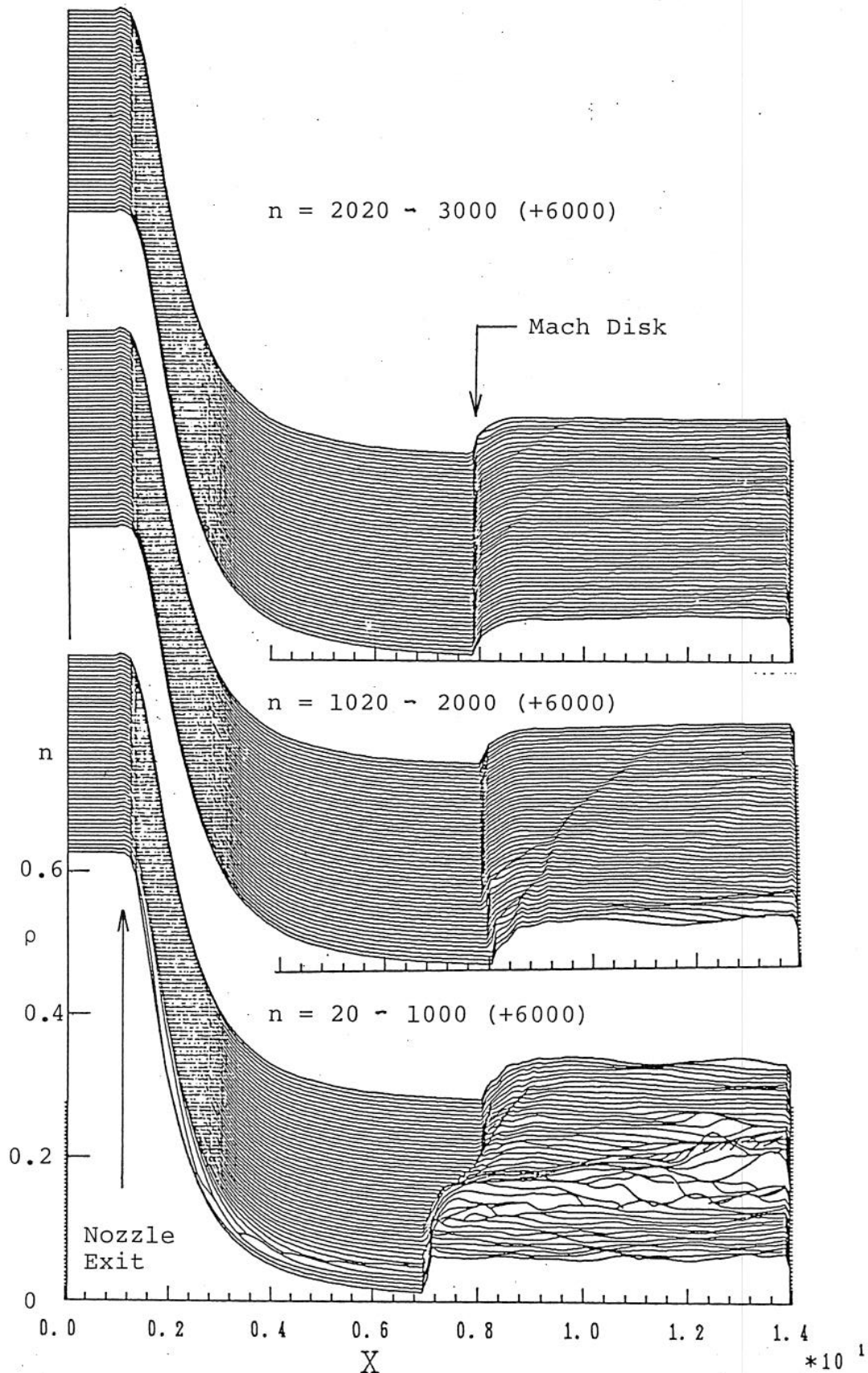


Fig. B-4 - 1

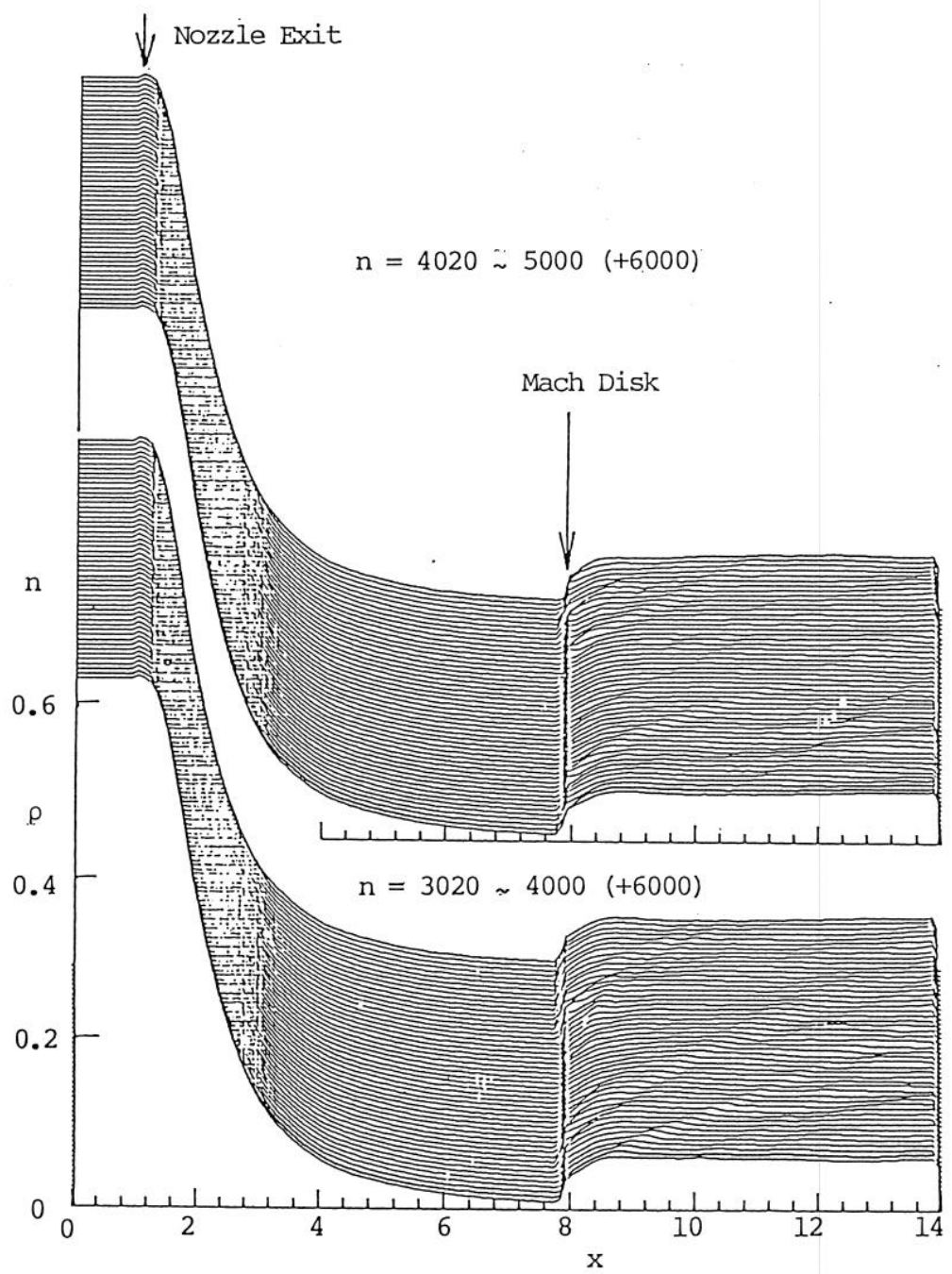


Fig. B-4 -2

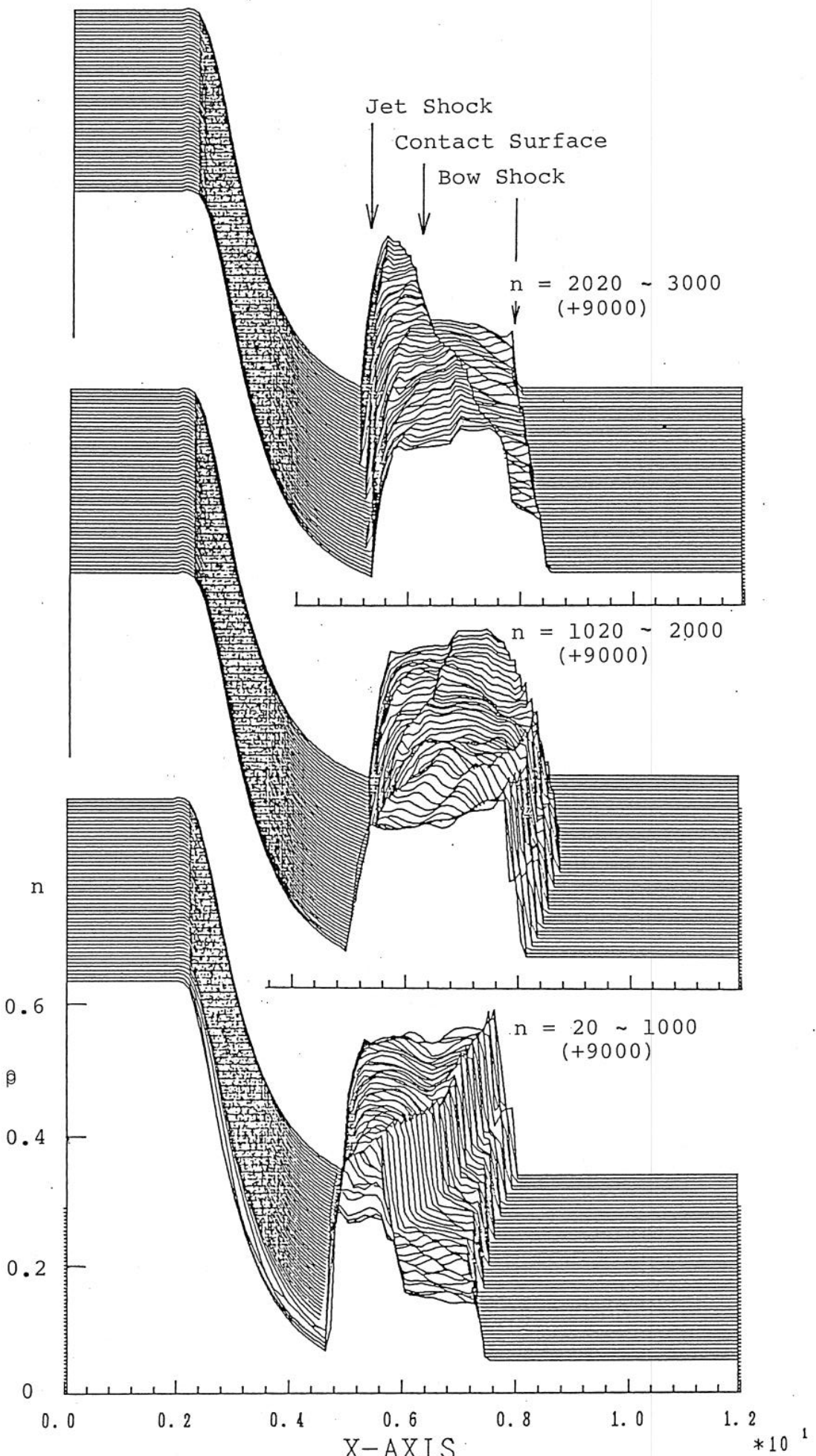


Fig. B-5-1

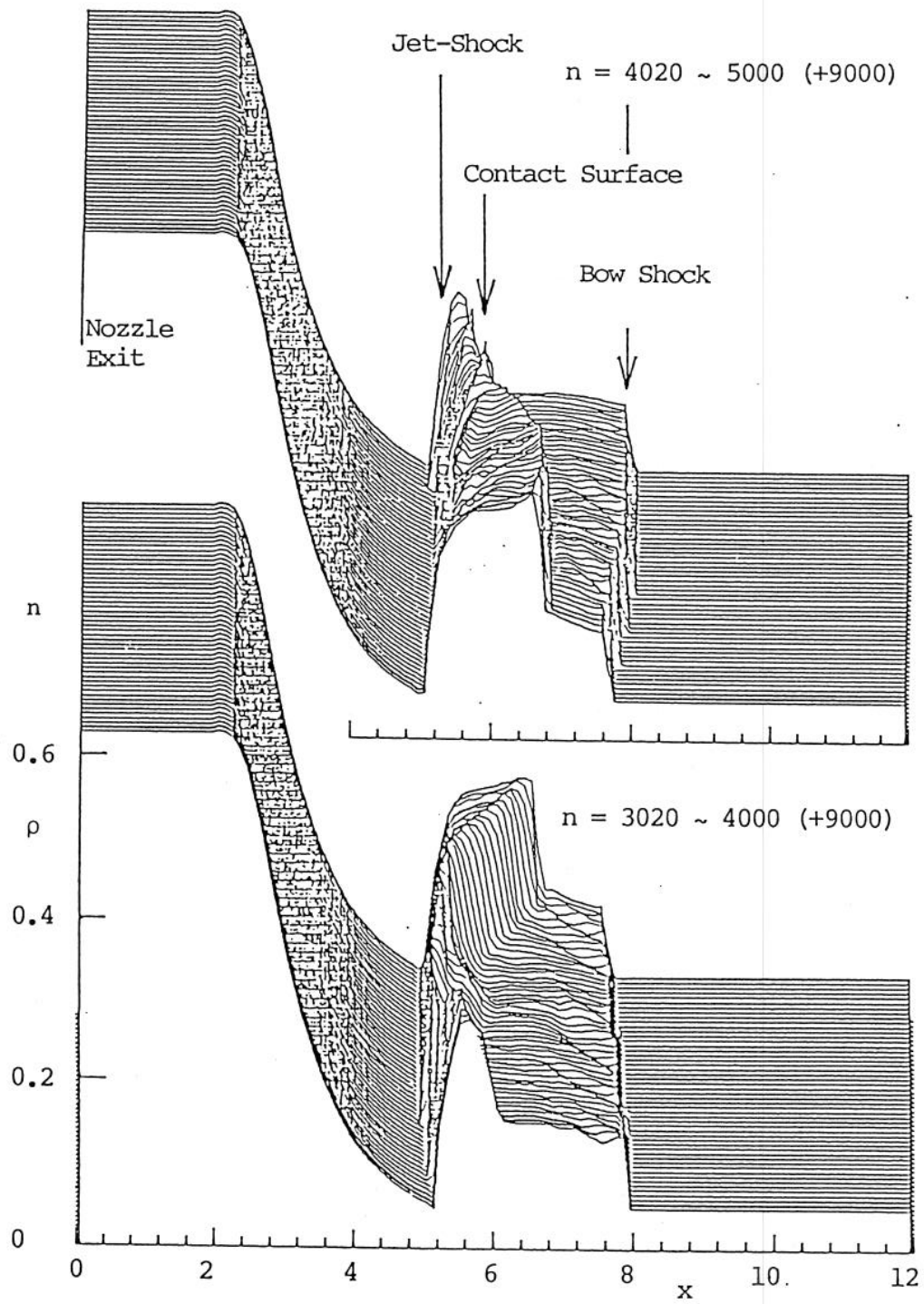


Fig. B-5 - 2

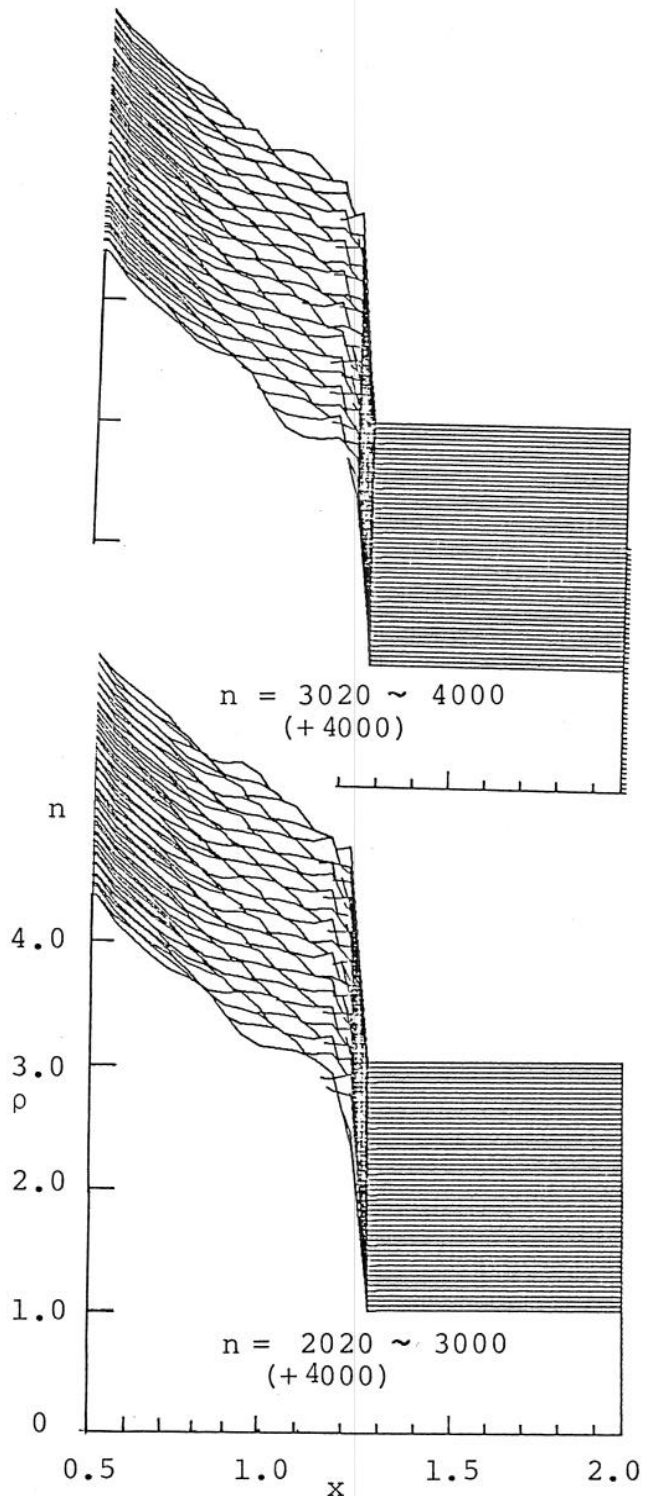
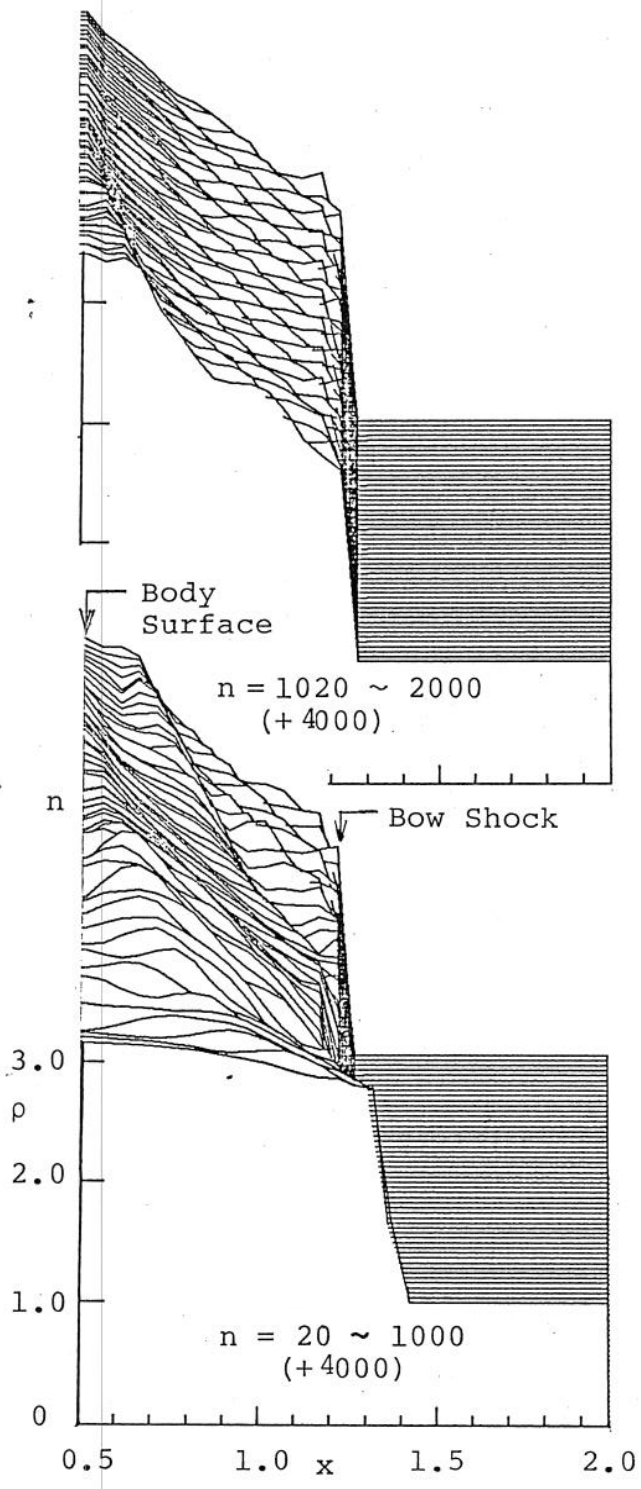


Fig. B-6

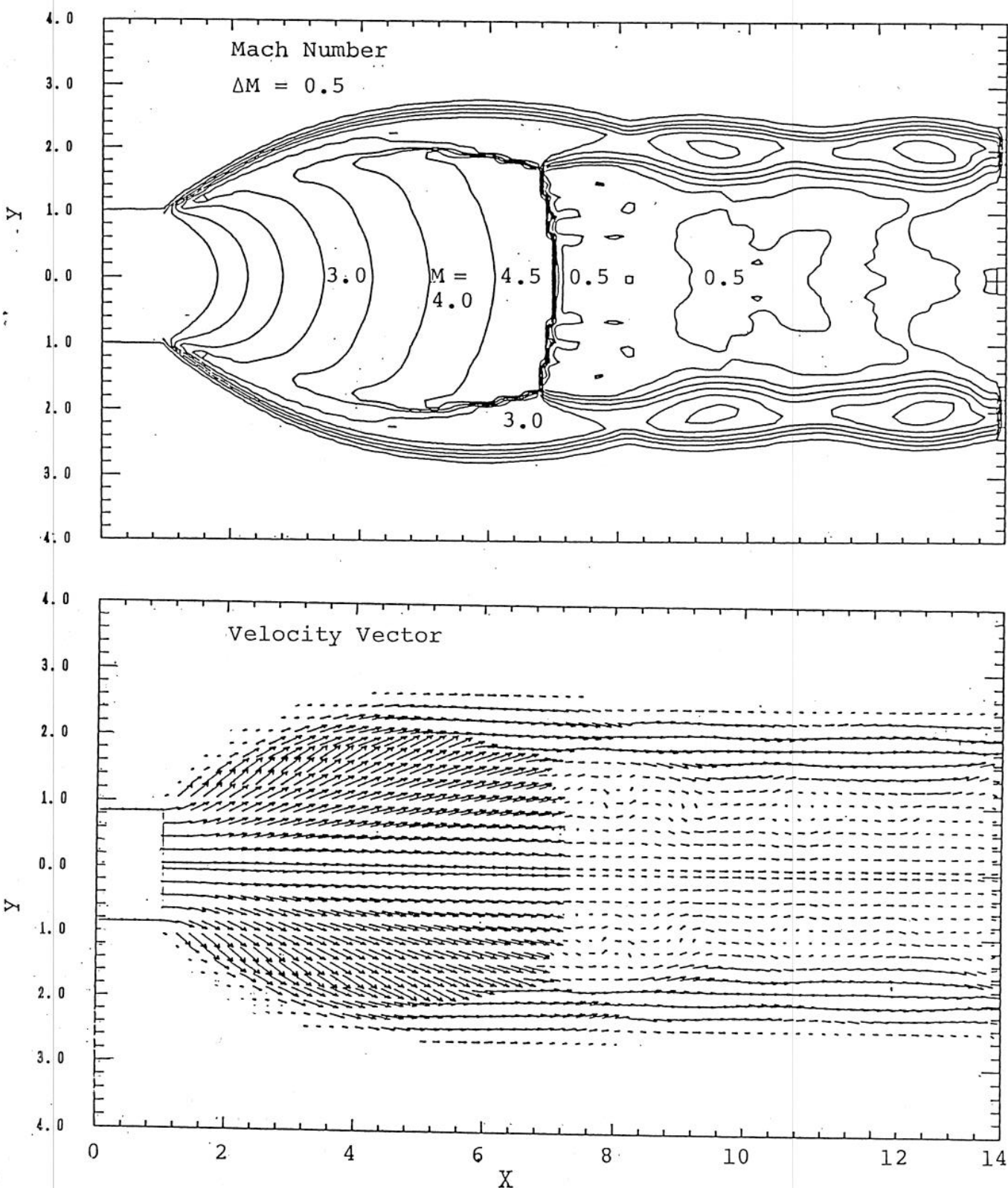


Fig. B-7

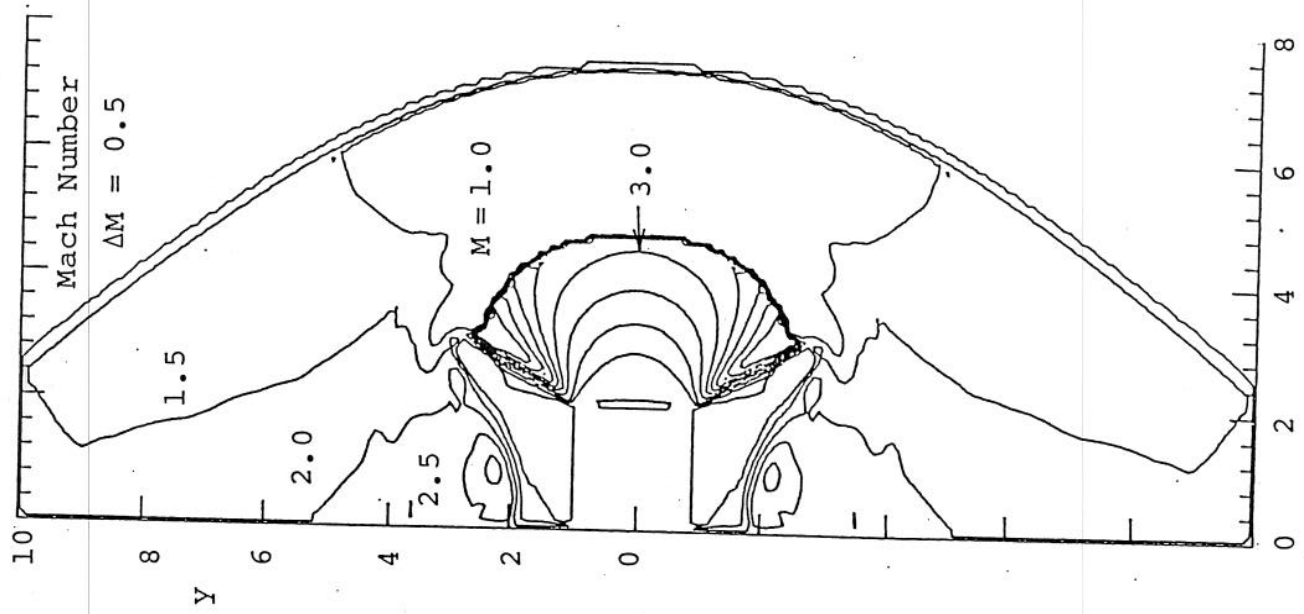
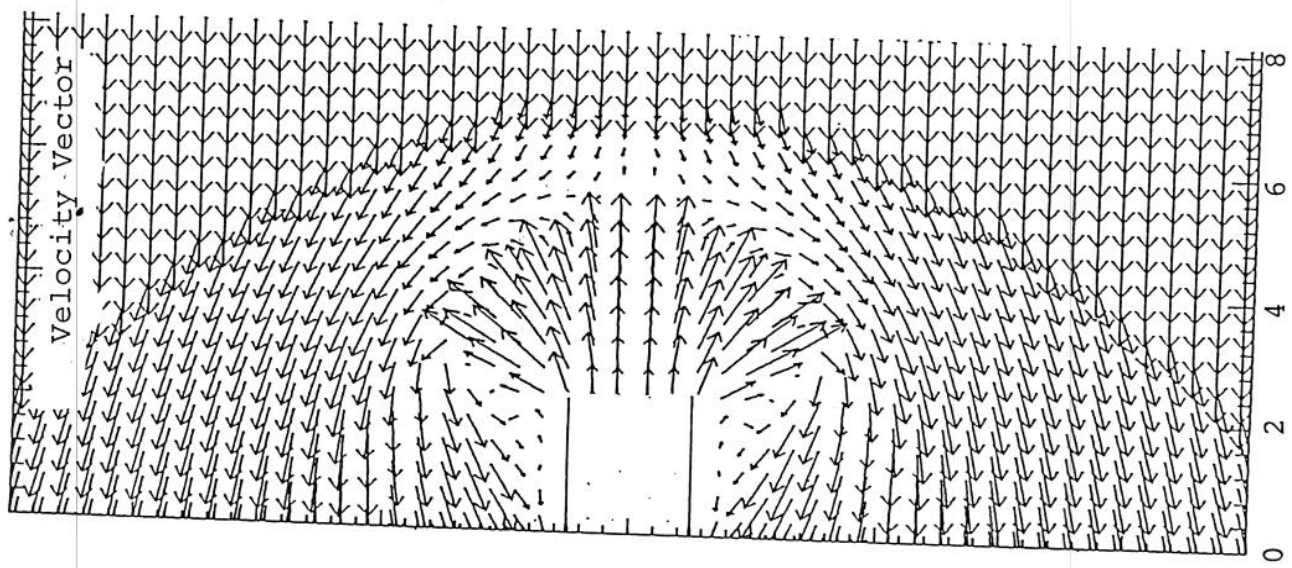


Fig. B-8

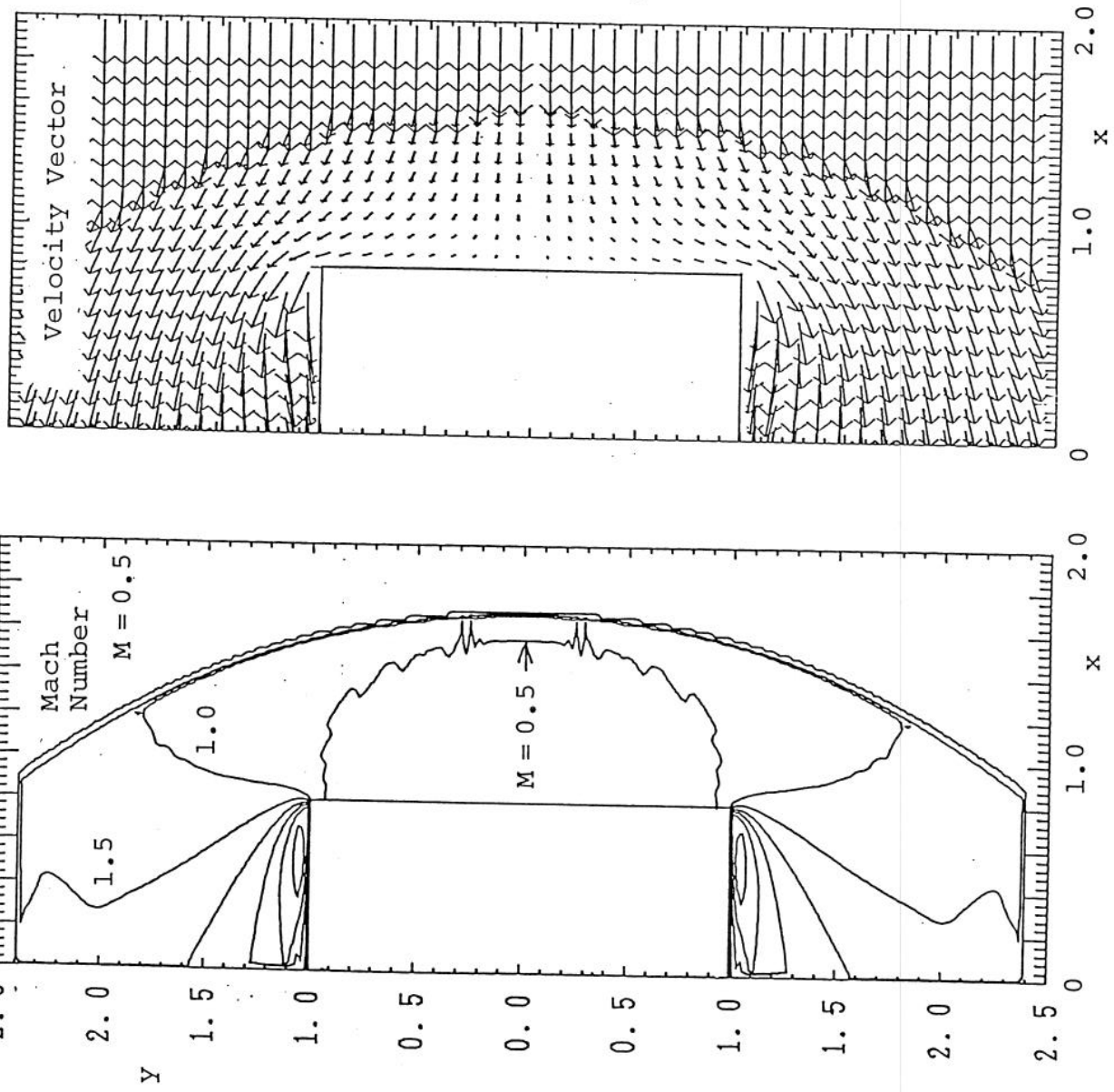


Fig. B-9 -1

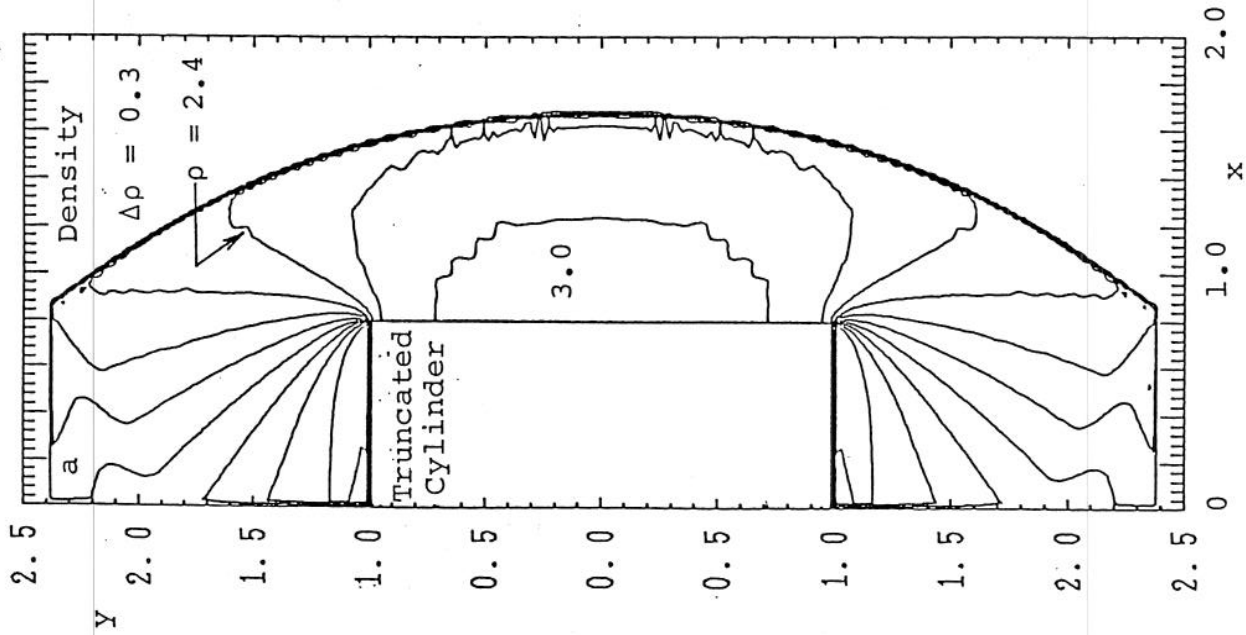
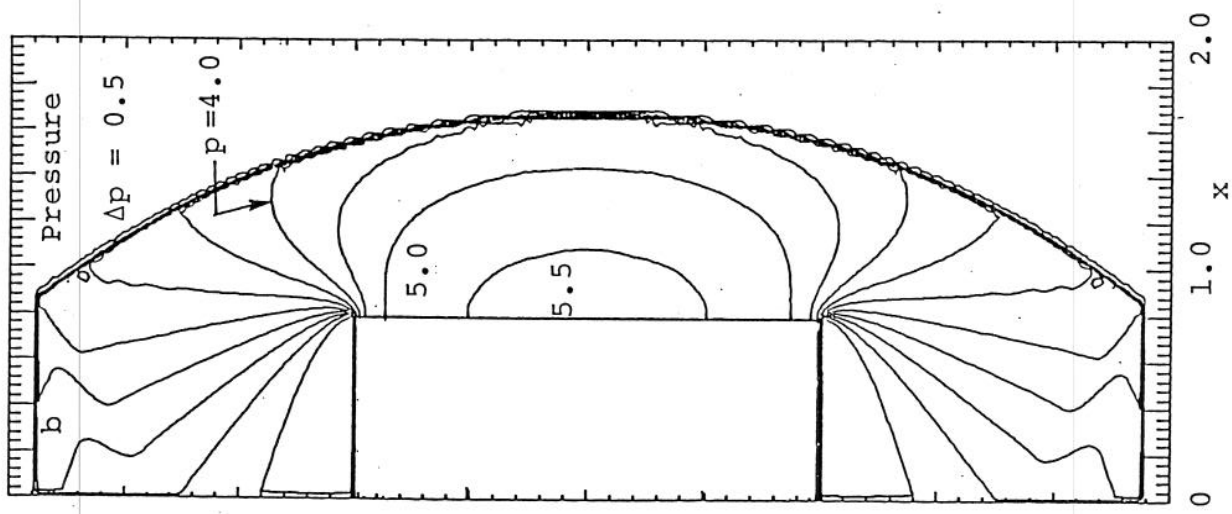


Fig. B-9-2

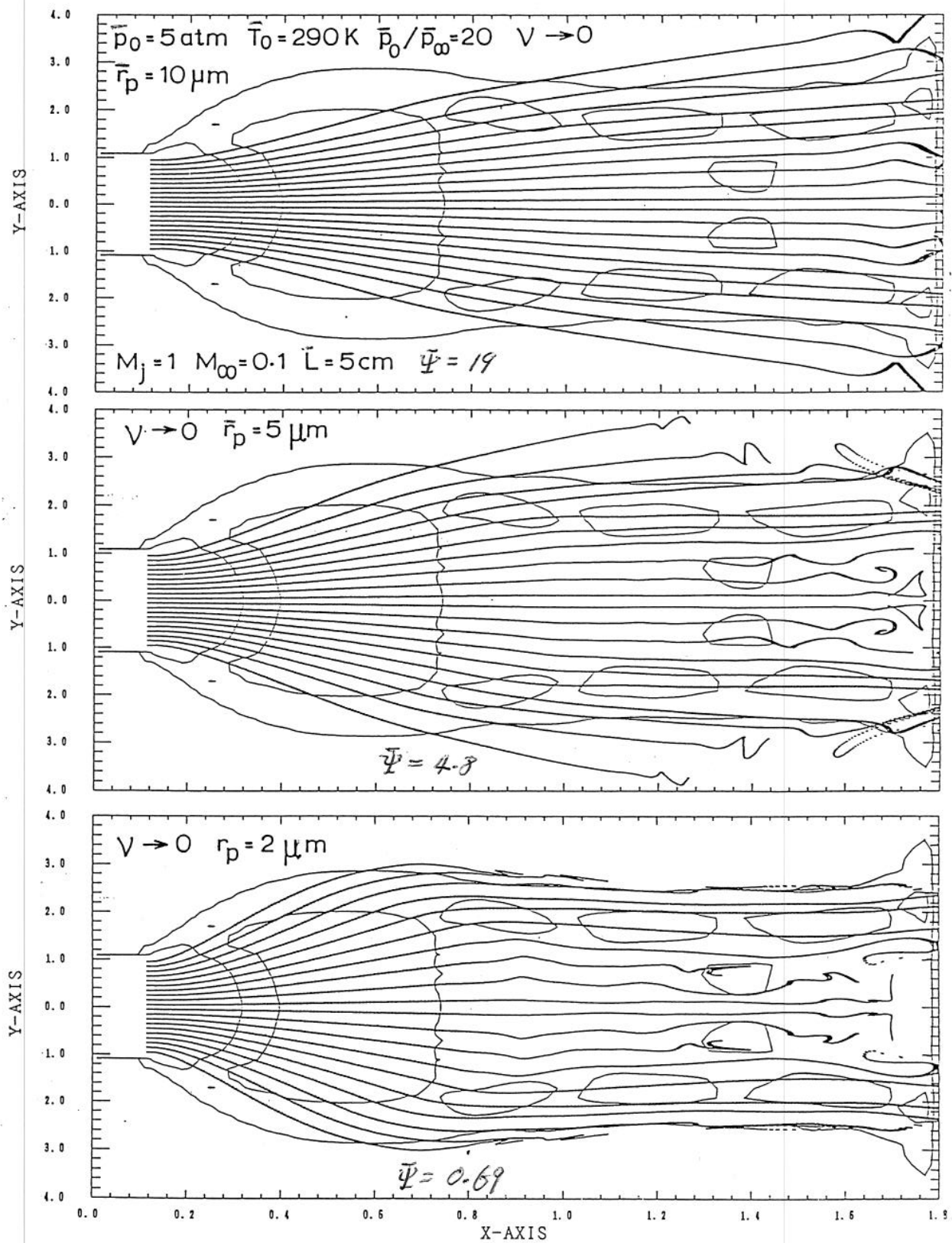


Fig. B-10 - 1

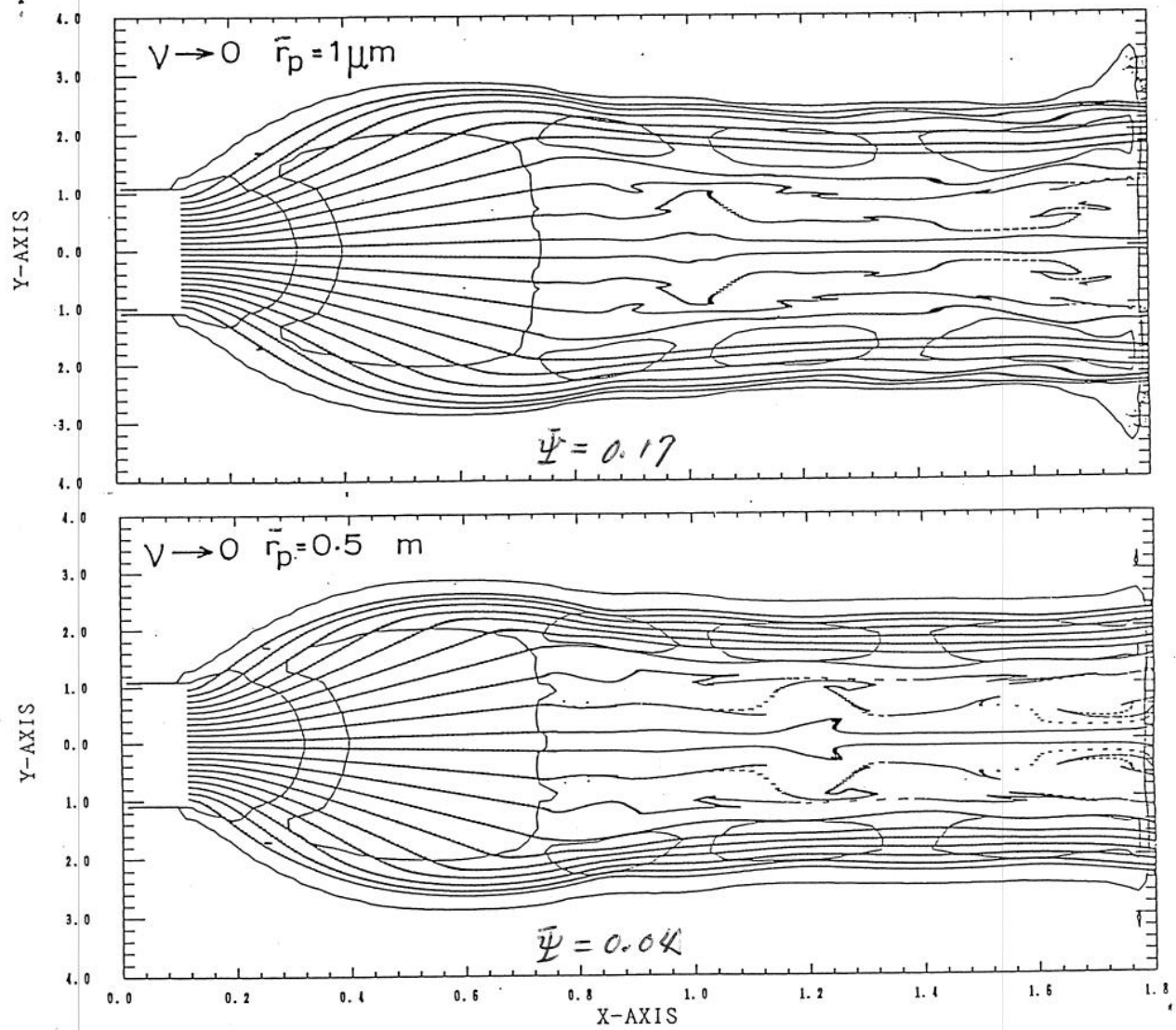


Fig. B-10 -2

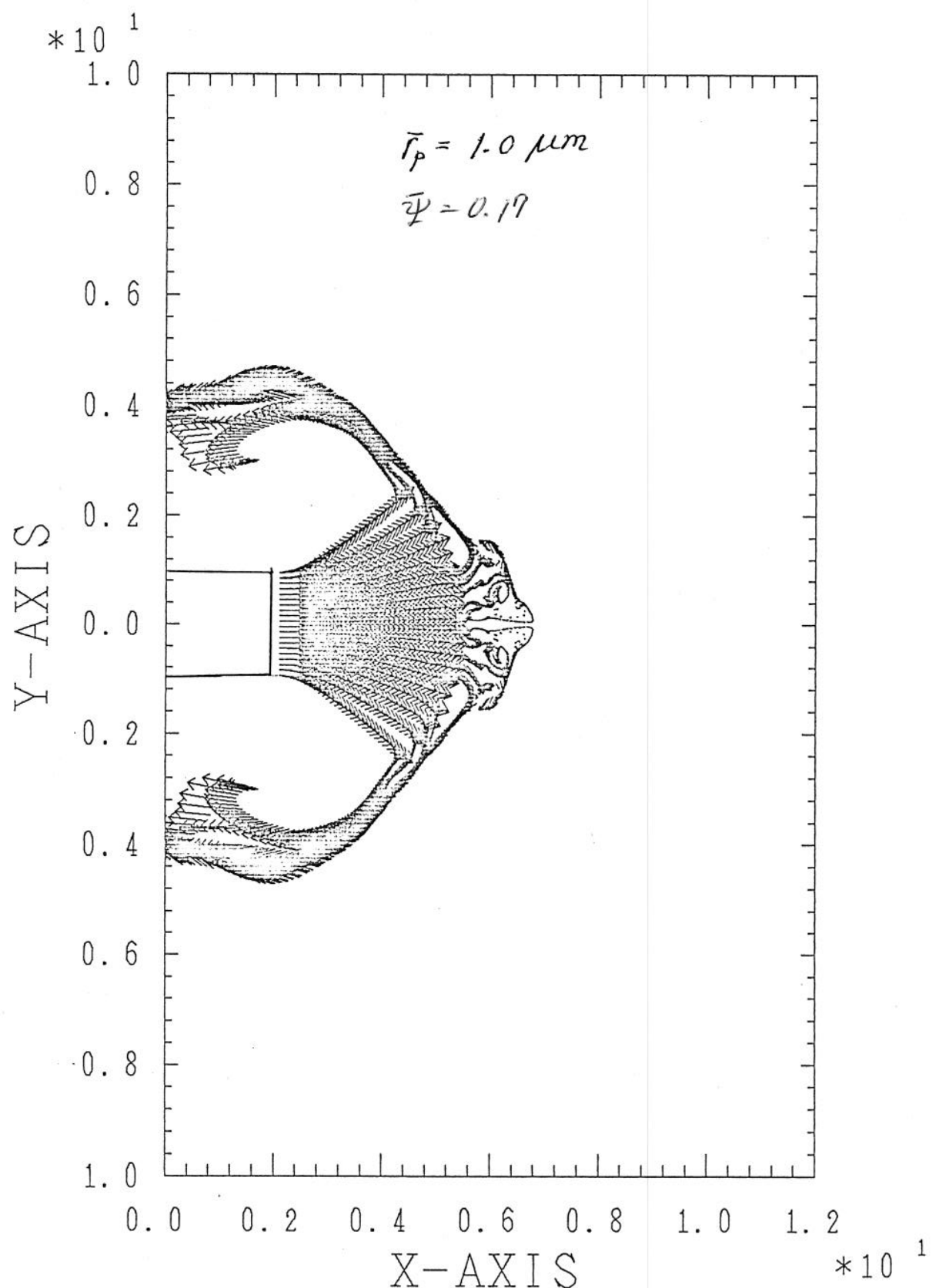


Fig. B-11-1

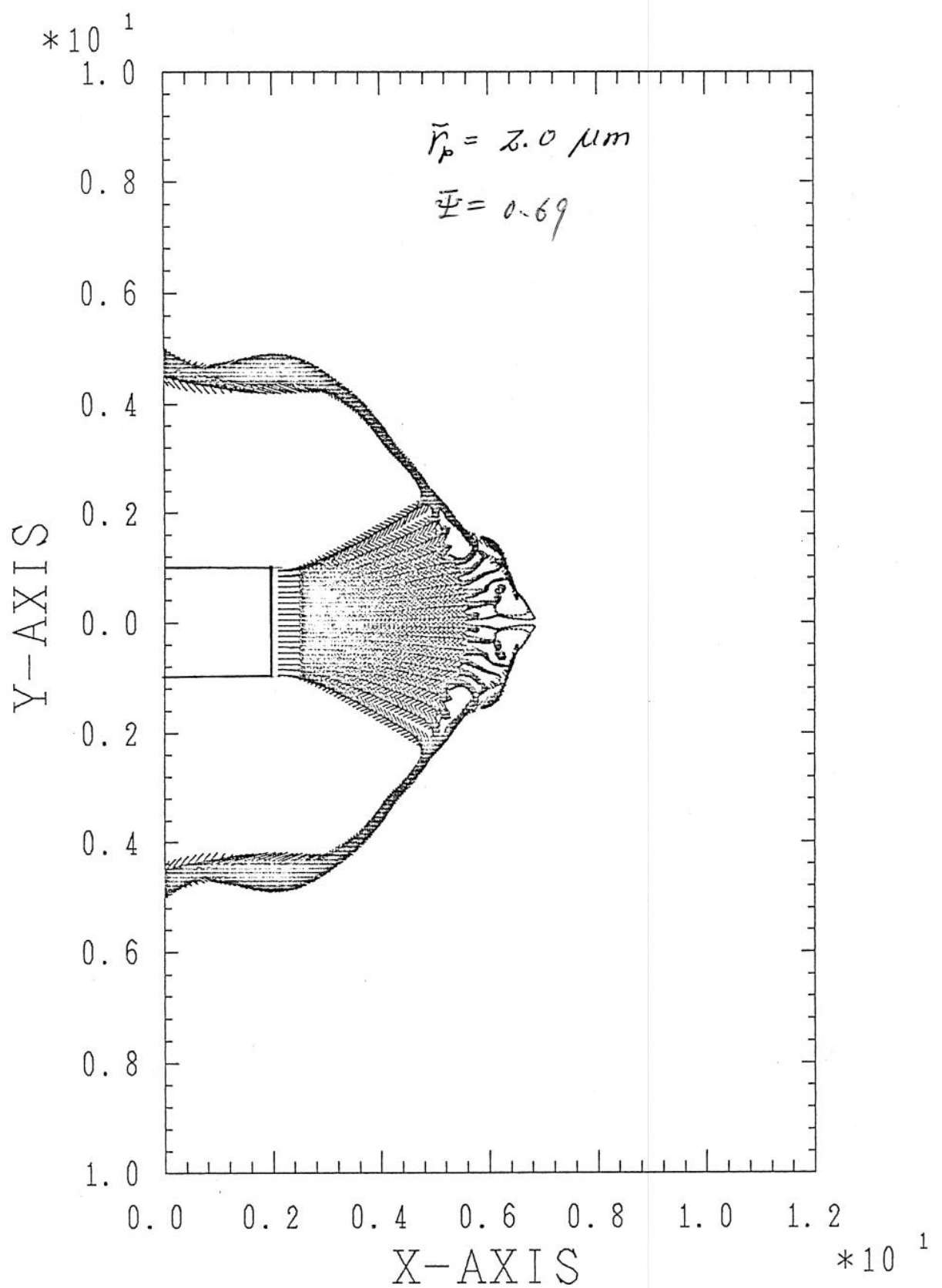


Fig. B-11-2

III

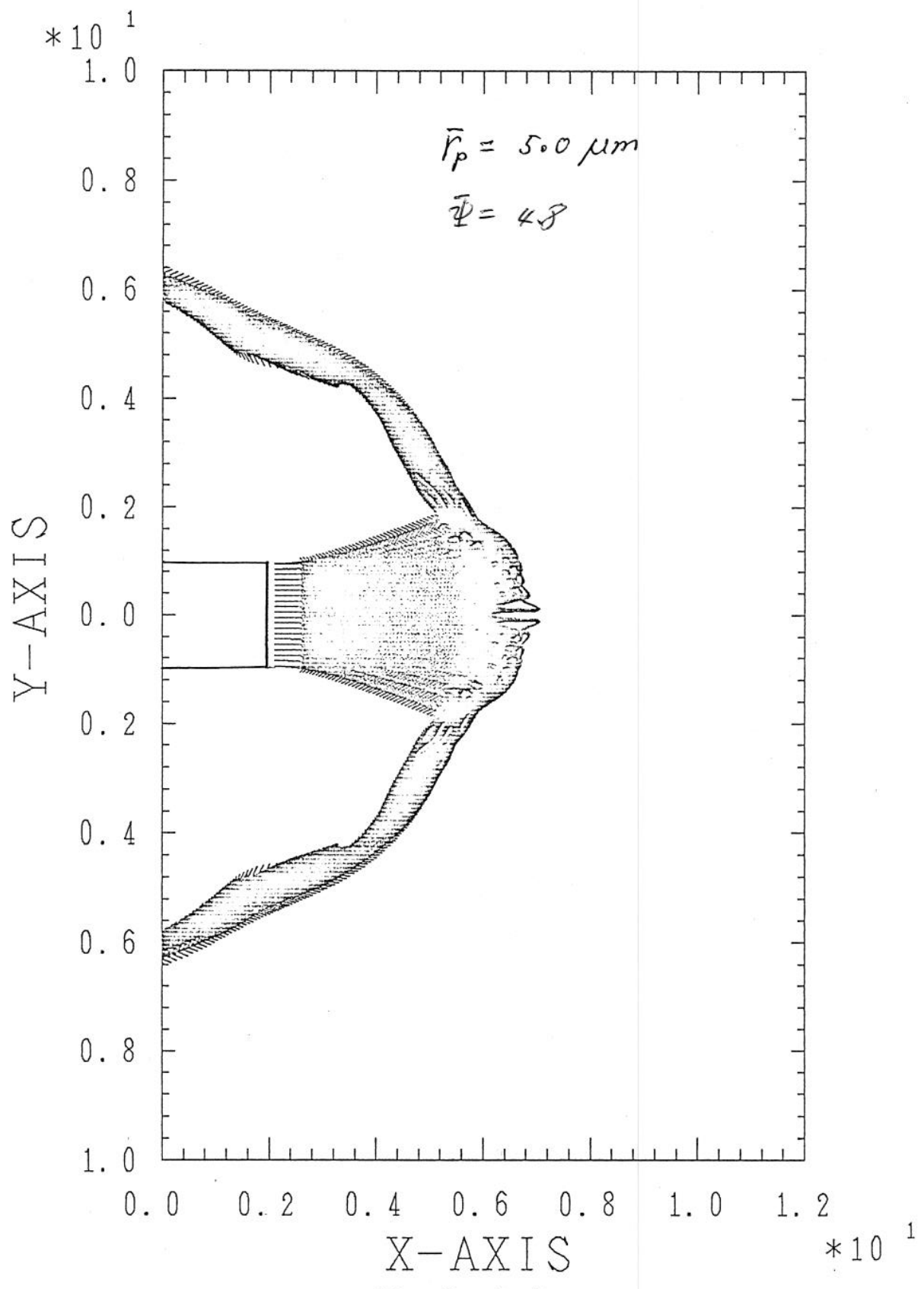


Fig. B-11-3

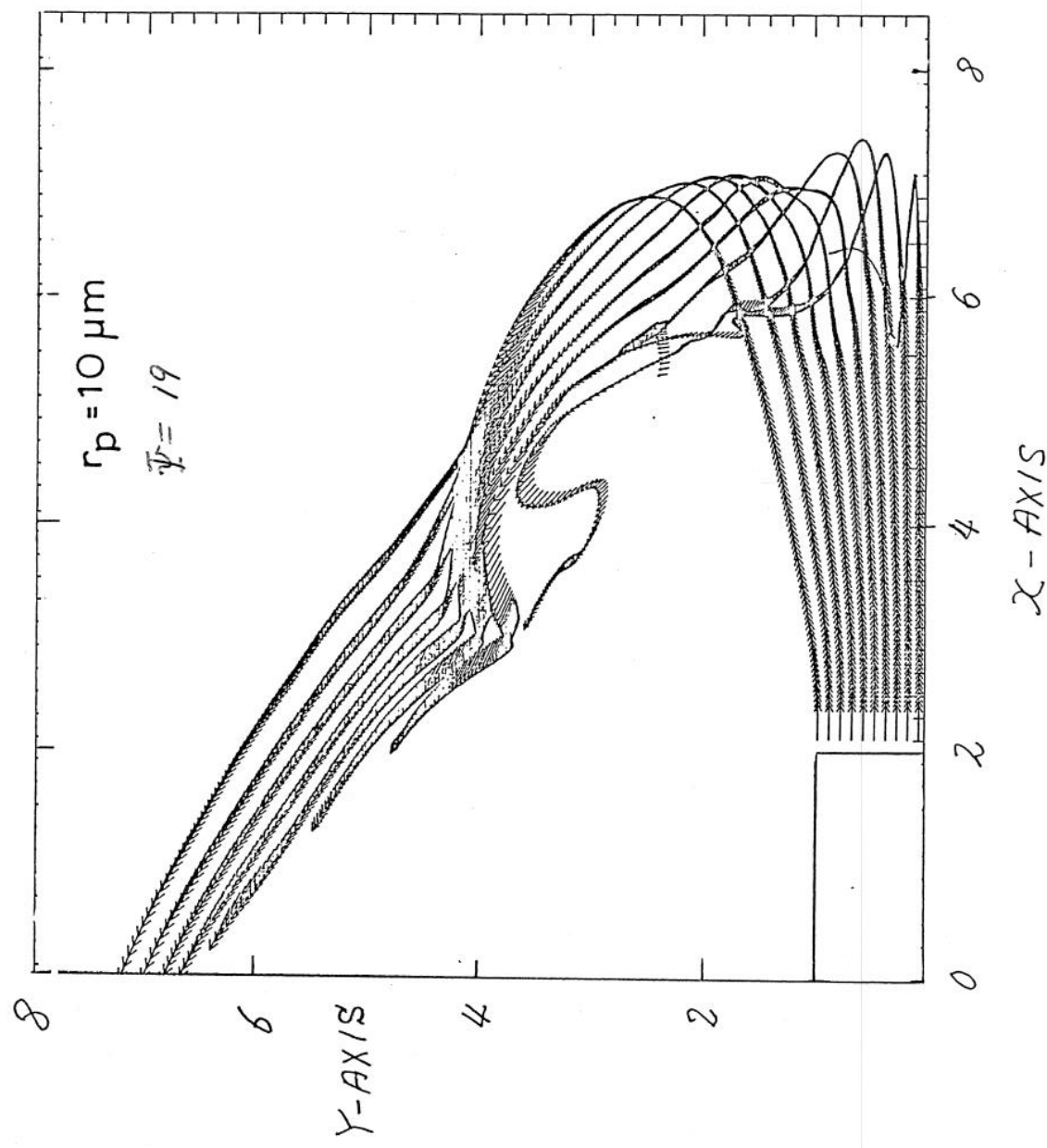


Fig. B-11-4

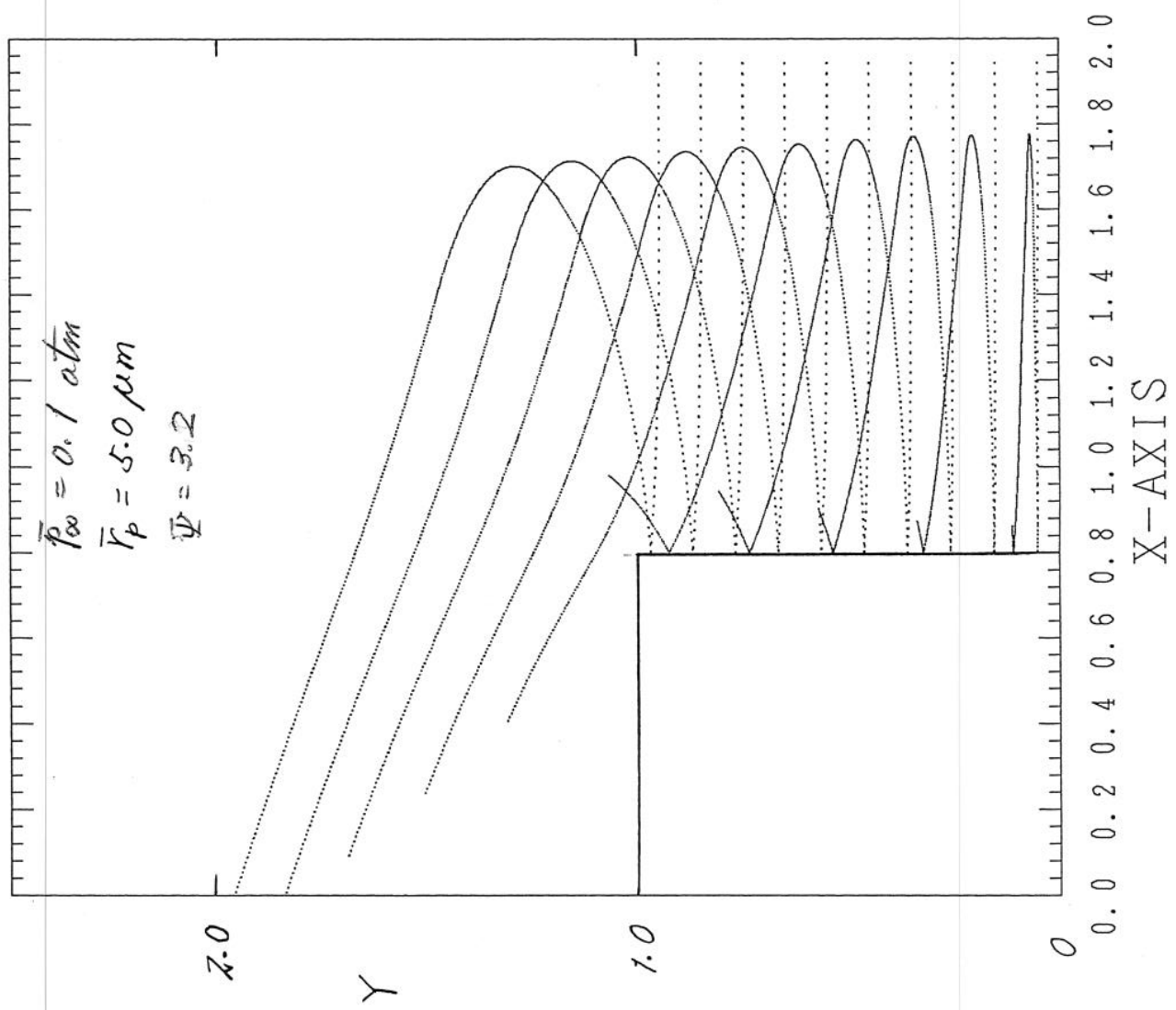


Fig. B-12

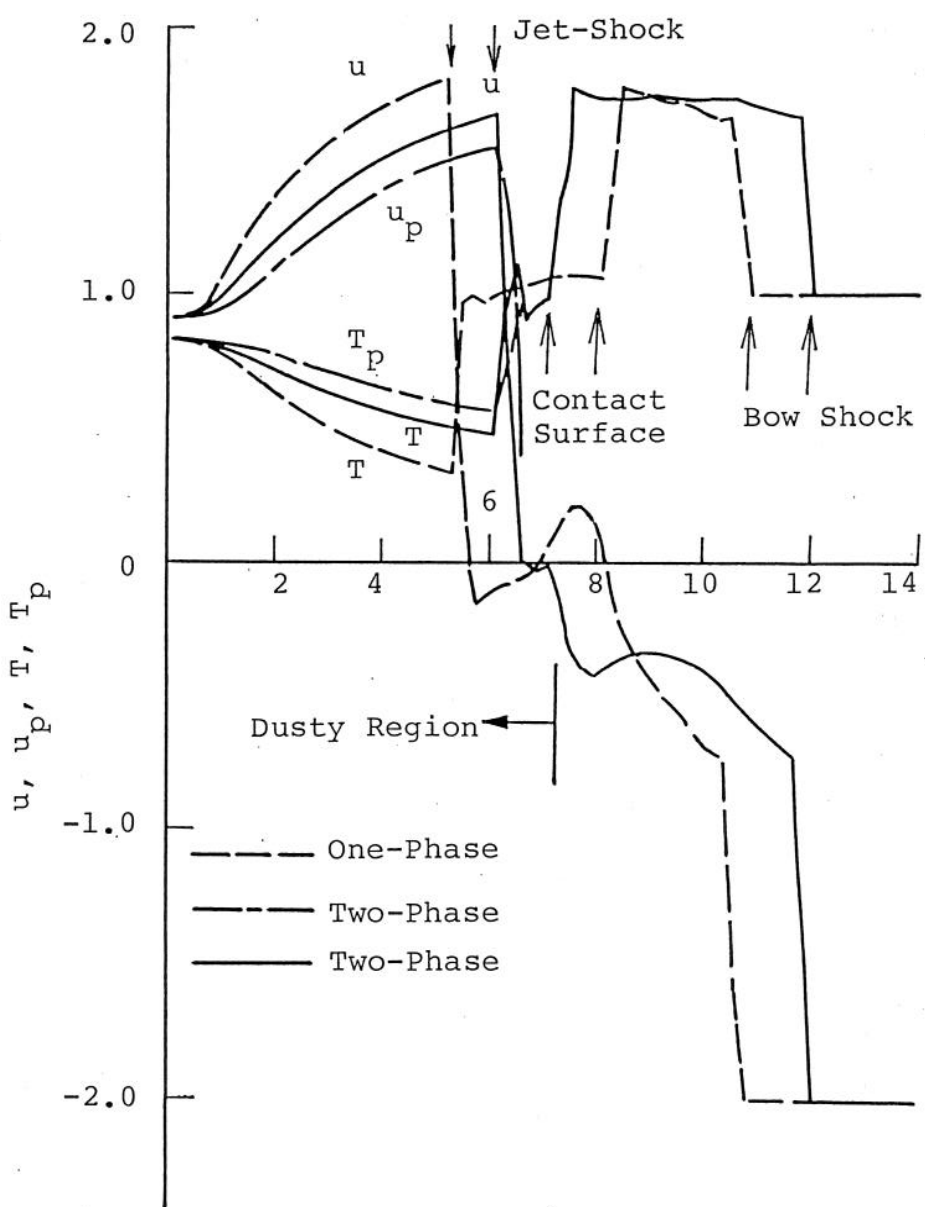


Fig. B-14

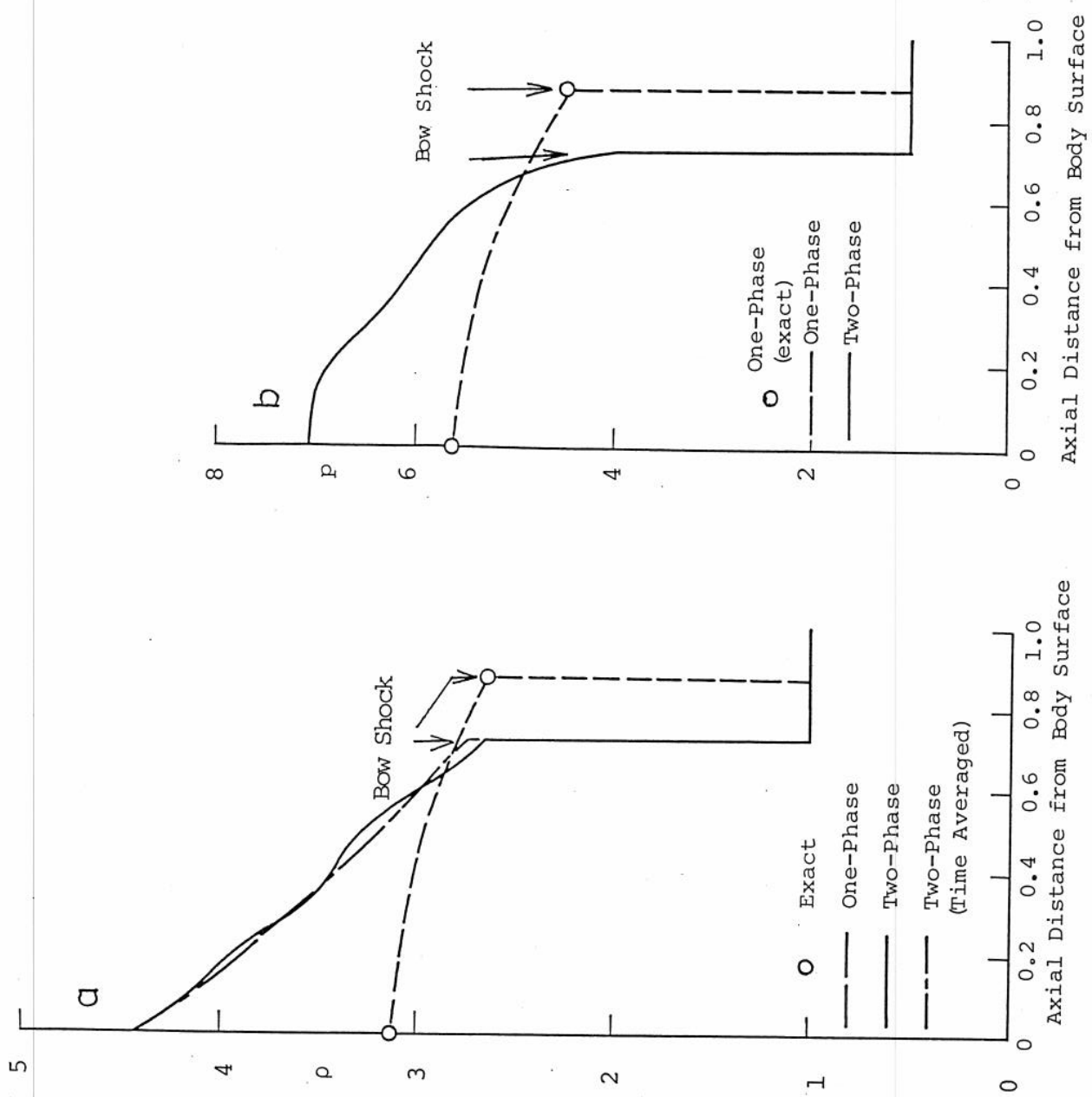


Fig. B-15-1

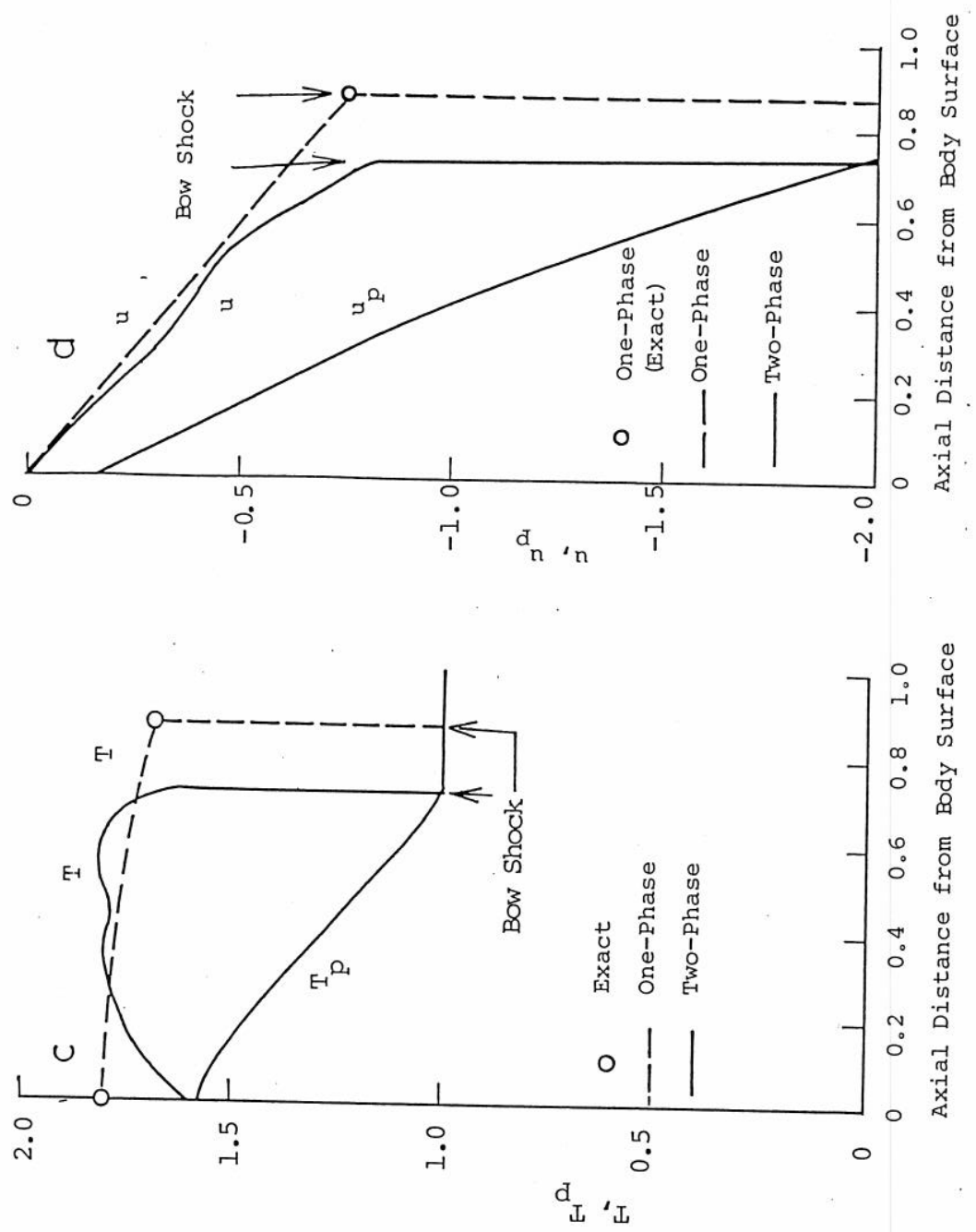


Fig. B-15-2

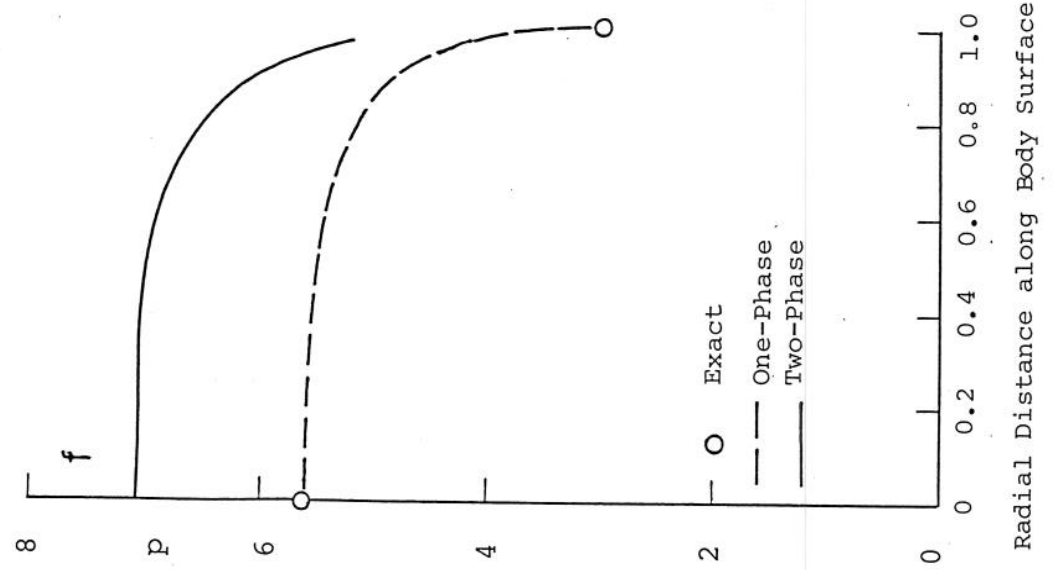
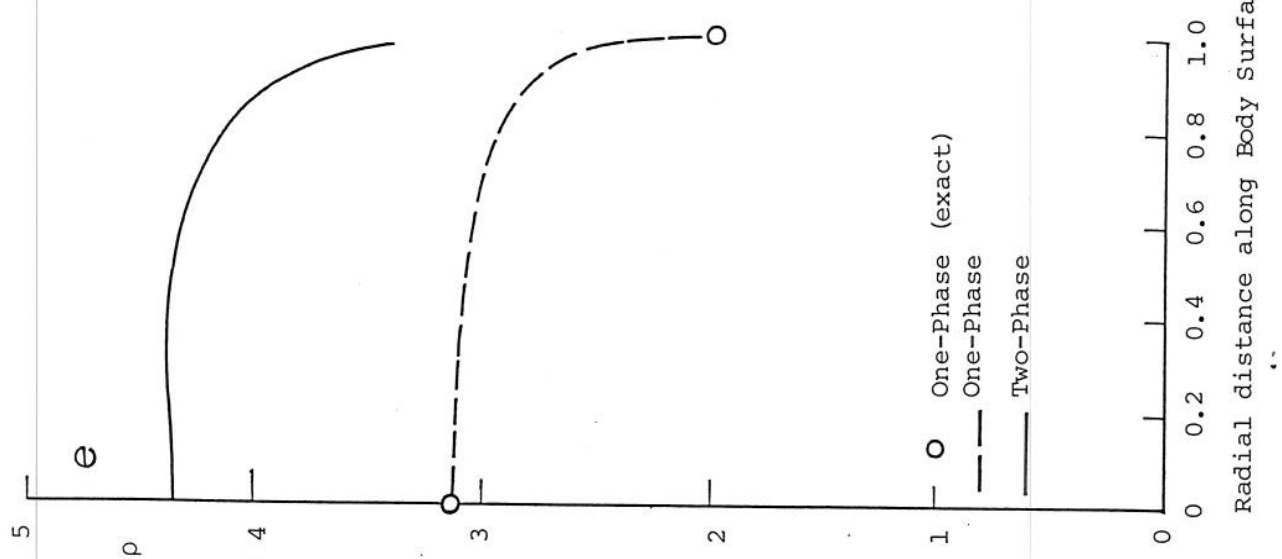


Fig. B-15-3

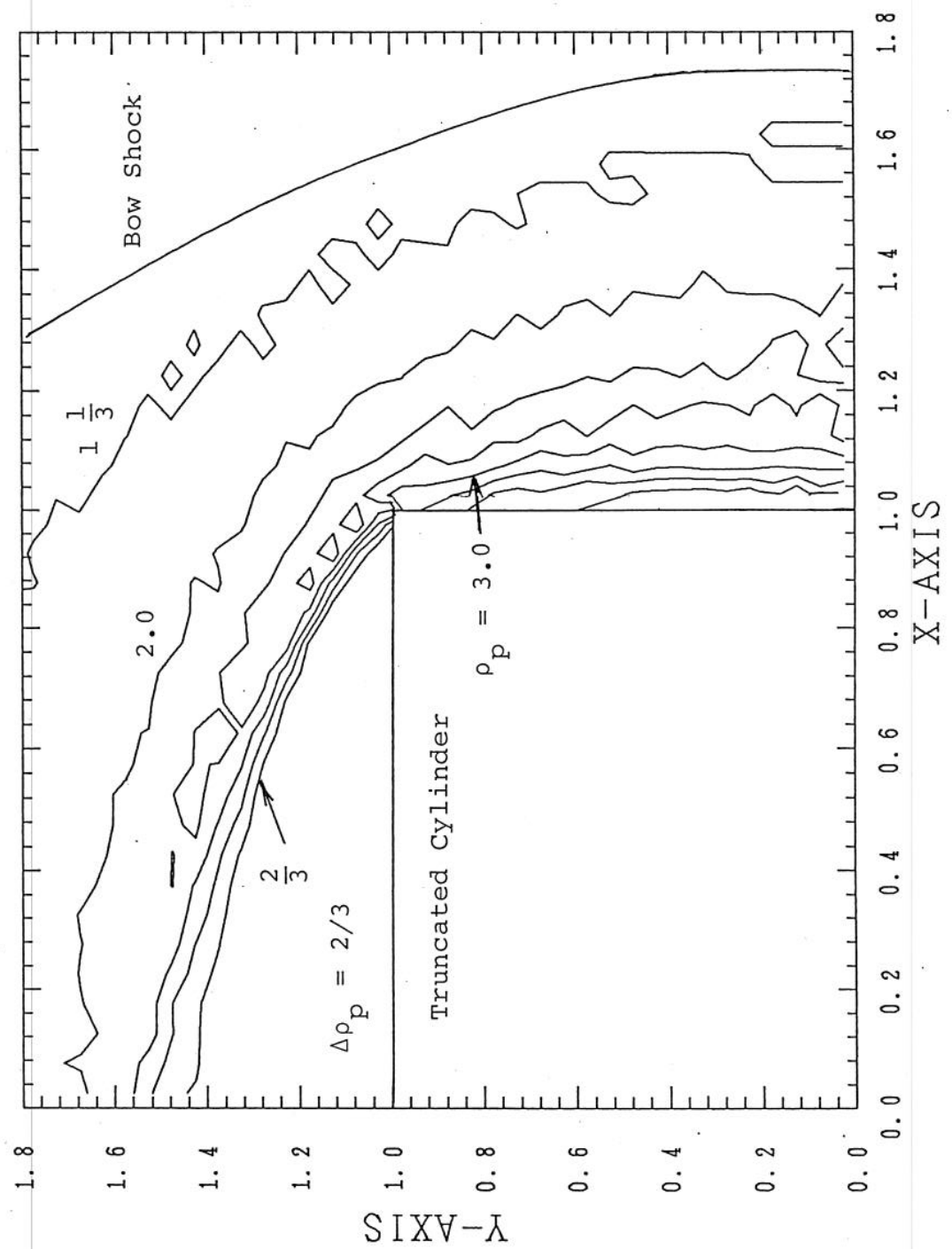


Fig. B-16

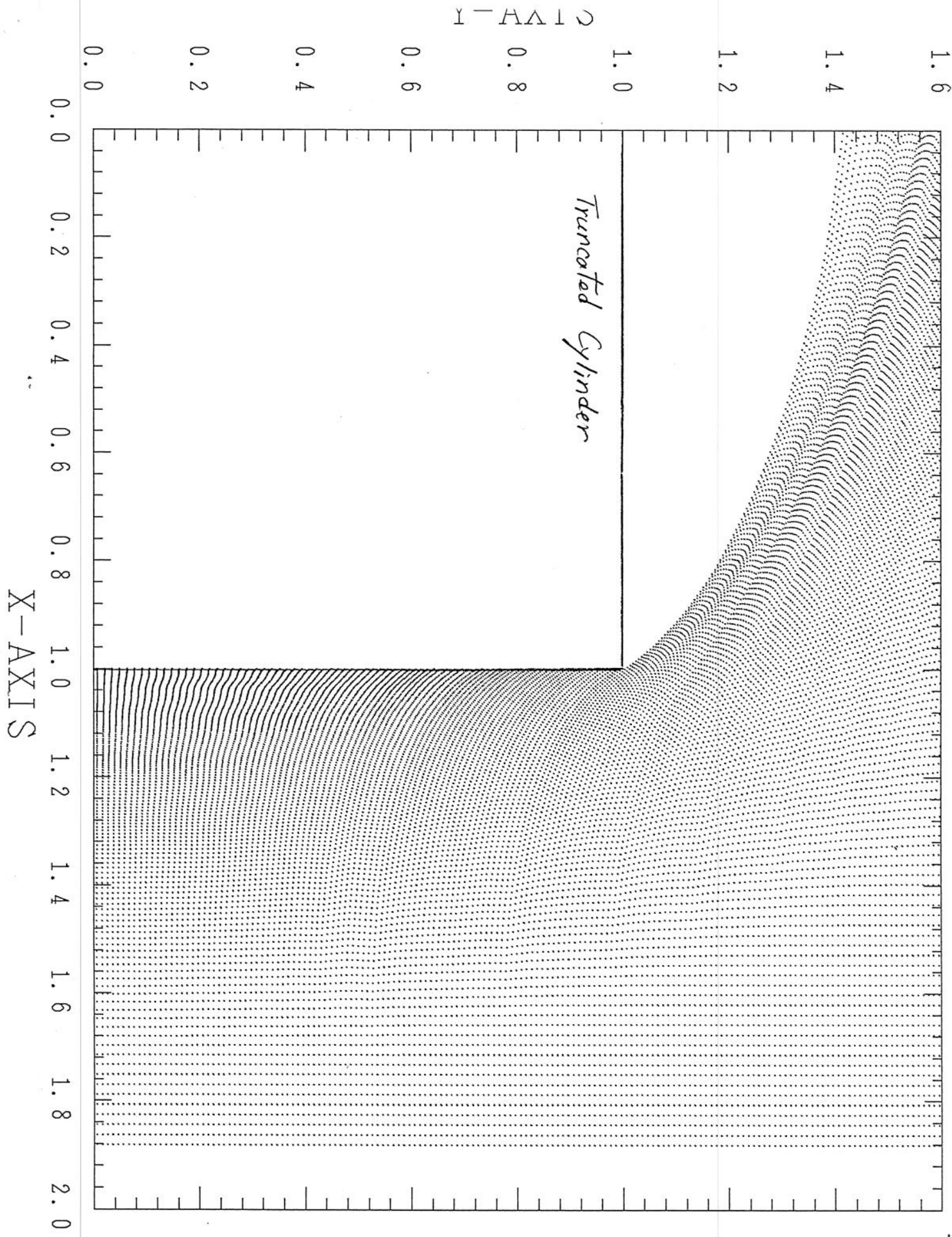


Fig. B-17